

Performance up gradation of static VAR compensator with thyristor binary switched capacitor and reactor using model reference adaptive controller

Swapnil D. Patil, Renuka A. Kachare, Anwar M. Mulla & Dadgonda R. Patil

To cite this article: Swapnil D. Patil, Renuka A. Kachare, Anwar M. Mulla & Dadgonda R. Patil (2022) Performance up gradation of static VAR compensator with thyristor binary switched capacitor and reactor using model reference adaptive controller, *Automatika*, 63:1, 26-48, DOI: [10.1080/00051144.2021.1999704](https://doi.org/10.1080/00051144.2021.1999704)

To link to this article: <https://doi.org/10.1080/00051144.2021.1999704>



© 2021 The Author(s). Published by Informa UK Limited, trading as Taylor & Francis Group.



Published online: 09 Nov 2021.



Submit your article to this journal [↗](#)



Article views: 795



View related articles [↗](#)



View Crossmark data [↗](#)



Performance up gradation of static VAR compensator with thyristor binary switched capacitor and reactor using model reference adaptive controller

Swapnil D. Patil ^a, Renuka A. Kachare ^b, Anwar M. Mulla ^c and Dadgonda R. Patil ^b

^aPh.D Research Scholar, VTU-RRC Belagavi and Electrical Engineering Department, Annasaheb Dange College of Engineering and Technology, Ashta, Maharashtra, India; ^bElectrical Engineering Department, Walchand College of Engineering, Sangli, Maharashtra, India; ^cElectrical Engineering Department, Annasaheb Dange College of Engineering and Technology, Ashta, Maharashtra, India

ABSTRACT

There are various static var compensator configurations are available and listed in the literature. Their performances are evaluated based on their voltage support, dynamic response, losses, cost, and additional filter requirement, if any. In this paper, efforts are made to improve the dynamic performance parameter such as rise time, settling time, and peak overshoots. A new topology with an adaptive controller is presented, in which capacitor and reactor banks are divided in their binary values and connected in the shunt. Capacitor and reactor banks are operated by thyristorised switches. Both these banks are operated in closed-loop form as a cascade control. Amongst these, capacitor bank operates as coarse control, and reactor bank acts as fine control. For the performance enhancement, a model reference adaptive controller is used. The system identification toolbox is used to evaluate the mathematical model of the plant with Matlab. The model's performance was analyzed deeply by the adaptive controller with different reference models such as critical, under, and overdamped. The performance parameters such as rise time, settling time, and peak overshoot in the form of reactive power swings, are evaluated and plotted for different adaptive gains using MIT rules.

Abbreviations: m_p : Peak overshoot; Q_C : Reactive power of capacitor; Q_L : Reactive power of inductor; $Q_{TBS C}$: Reactive power of TBSC bank; $Q_{TBS R}$: Reactive power of TBSR bank; t_r : Rise time; t_s : Settling time; e : Error; $G_c(s)$: Transfer function of TBSC plant; $G_r(s)$: Transfer function of Disturbance plant; $G_r(s)$: Transfer function of TBSR plant; SVC: Static VAR Compensator; t : time; TBSC: Thyristor binary switched capacitor; TBSR: Thyristor binary switched reactor; TSC: Thyristor switched capacitor; TSR: Thyristor switched reactor; $u(t)$: System input; $v(t)$: System disturbance; $y(t)$: System output; Y_m : Reference model output; Y_p : Plant output; γ : Adaptive gain; θ : Theta

ARTICLE HISTORY

Received 2 February 2021
Accepted 20 October 2021

KEYWORDS

Binary switched capacitor and reactor; reactive power; model reference adaptive controller; performance parameter; system identification

1. Introduction

The electricity demand increases day by day, and fulfilling it requires installing a new generating station with a transmission and distribution network. But the installation of a new generating station in the existing power system network becomes costly and less feasible. Also, nowadays, the use of renewable energy sources in power systems is increasing rapidly and integrated with the grid. It creates new challenges in the power grid regarding the dynamic variation in power-frequency (P-f) and reactive power-voltage (Q-V) control problems. Also, power electronics devices like converters for grid integration and controllers in charging stations of electric vehicles in smart grids cause dynamic variation, leading to power quality problems. It is not limited to this, but the distributed generation (DG) in the microgrid gives a poor performance in reactive power-sharing. Because in the microgrid, the reactive power of each distributed generator depends on the load active

power. There is a need to maintain the balance between generation and utilization of power along with fulfilling the demand of reactive power in the microgrid. The dynamic variation in voltage because of poor management of reactive power-sharing in the microgrid can be resolved through upgrading the existing system by reducing losses, improving efficiency, and enhancing the power transfer capability of the system, which will give a better solution.

To achieve these, there are different types of FACTS controllers like shunt and series-connected static VAR compensator, static synchronous compensator (STATCOM), unified power flow controller (UPFC), and interline power flow controller (IPFC), phase angle, and voltage regulator are available. All these devices are used with ordinary PI or advanced controllers with a closed-loop system. Because systems are already heavily loaded, it requires maintaining system stability at the steady-state and dynamic disturbance in the

power grid. The FACTS controllers with a proper controller like PID, fuzzy logic controller, model predictive control (MPC), model reference adaptive controller (MRAC), etc., are the best controllers, which gives good performance at transient and steady-state conditions in the power grid. Such types of controllers help to improve the performance of FACTS devices to maintain system stability.

In [1], the emerging use of renewable energy sources in the electrical power grid is increasing day by day, and it creates new challenges in the power grid regarding active power-frequency (P-f) and reactive power-voltage (Q-V) stability problems which aggravate power quality problems too. These problems mainly arise due to the extensive use of power electronic devices for grid integration with renewable energy sources and nonlinear loads [2]. The FACTS device plays an important role in maintaining system stability and improving the grid's power quality. Also, in [3], a survey on control strategies like MPC, PI, PID, Fuzzy control, damping controller, integral linear Gaussian control are investigated to resolve the problems which arise microgrid integration with renewable energy sources. A comparison of static VAR compensator and static synchronous compensator with the fuzzy logic controller is used for wind farm integration in power system is presented in [4]. The fuzzy logic controller is used to damp out oscillation in an integrated system, and also the dynamic performance of the controller is investigated and concluded that the performance of fuzzy controller with static VAR and static synchronous compensator is improved with less peak overshoot. In microgrid distributed generator gives a poor performance in reactive power-sharing. Because the reactive power of each distributed generator depends on the active power load in the microgrid. To improve the performance of reactive power sharing concern to the microgrid, a droop control method of reactive power-sharing is analyzed and presented [5].

In the power grid, different application of predictive model control (MPC) has presented in the literature. The use of MPC for power oscillation and transient stability [6,7], transient voltage collapse by voltage control with MPC, and protection of the power system [8,9] has been proposed. In [10], multi-objective MPC-based SVC is presented, and the objective of this paper is to damp out oscillation and maintain voltage profile at the desired level with MPC-based SVC. In [11] adaptive voltage controller based on double sliding mode strategies for SVC is used. The SVC with such a controller is used in an isolated power system with wind and diesel generation to control voltage in an isolated power system. In [12,13], the mathematical modelling of MPC-based SVC with a multi-objective function prevents voltage fluctuation, oscillation, and collapse is presented. Also, In [14], two different strategies are presented. The first strategy is the static load shedding

algorithm, and the second is associated with trajectory sensitivities. In [15,16], the traditional static var compensator based on a PI controller is designed for an isolated power system under different conditions. GA and ANN with an optimized PI controller are presented in [17–19] to control voltage instability. However, the PID controller gives reasonable results with the genetic algorithm method for tuning the PID parameters. The different configurations based on the binary switched capacitor with fixed tuned PI controller parameter is presented in [20–23] to compensate for the rapid variation in the reactive power for different loading conditions. To compensate for reactive power and control voltage in the power system, SVC will be an economical solution [24,25].

In [26], STATCOM, along with MRAC, is presented to enhance the performance of the grid with wind energy integration. But considering the cost, STATCOM is costlier than SVC [27], adaptive controller with an observer from SVC presented in [28,29]. The system's behaviour can vary significantly between loading conditions like Q-V (reactive power and voltage) and P-F (power and frequency) variations. The controller used for such a condition may fail or be unable to perform optimally. Therefore the design of the controller is essential to perform optimally with different operating conditions. In [1], the paper presents the mathematical modelling of model reference adaptive controller (MRAC) based VAR compensator.

The analysis and impact of static var compensator with additional modern controllers used from the different perspectives of engineering problems are presented in [30]. Also, analysis of different controllers like traditional PID, Deformation of PID, Non-linear H_{∞} , variable structure control, optimum variable range control, backstepping control, intelligent control, and inverse system control was reported with a different engineering problem. The dynamic response of TCR-based compensator is not sufficient for dynamic reactive power compensation. That's why a new TCR-based compensator with feed-forward adaptive control method is used to minimize the demand of reactive power from the microgrid is presented [31]. Several shunts compensating devices are present to improve power quality and maintain voltage stability in the power system. But, each has one or other drawbacks like voltage support, dynamic response, harmonic generation, additional filters requirement, losses, and cost, which are presented in graphical form in Figure 1, which was discussed in [27, 32–38]. These outcomes of the compensator are summarized as the magnitudes versus the outcome parameter in the range on 0 to 5, which denotes as; “0” = Zero/Not Required; “1” = Very Low; “2” = Low; “3” = Moderate/Required; “4” High; “5” = Very High.

It is observed that there is no one method as an optimum. Keeping these performance parameters and

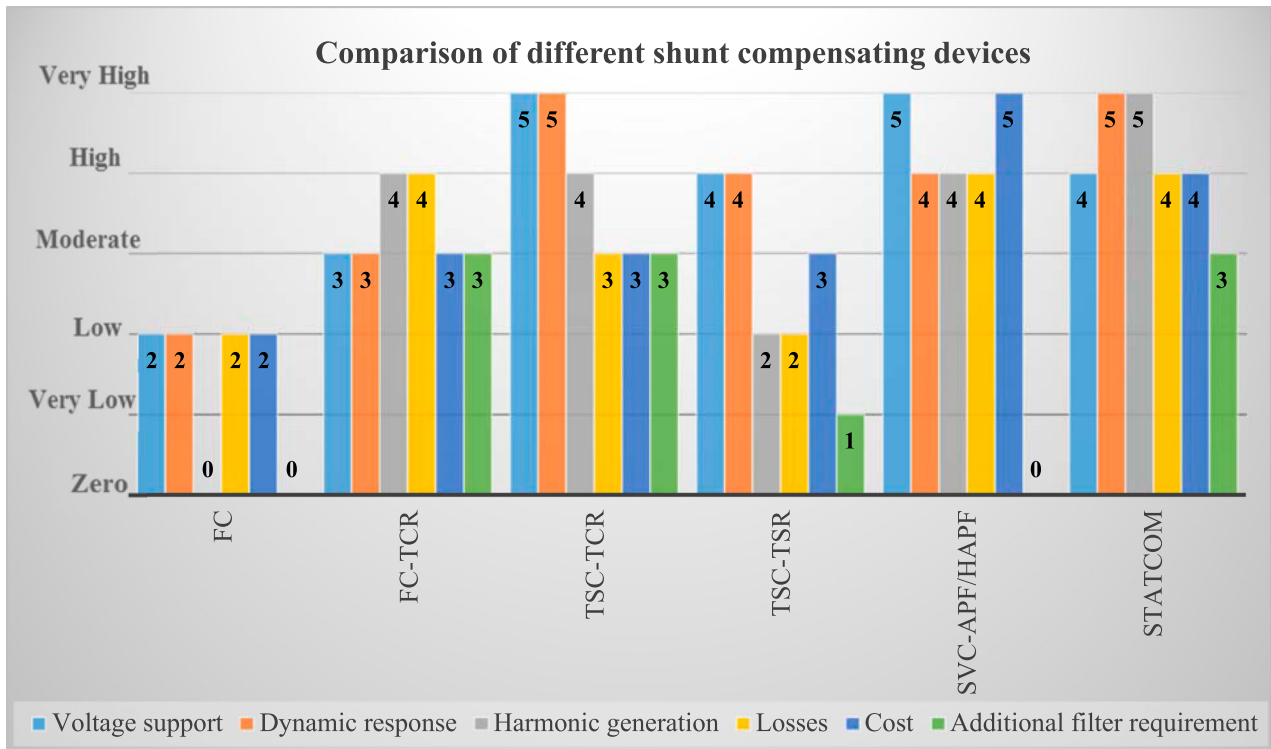


Figure 1. Outcome summary of different shunt compensating devices.

outcome of the compensators, a new topology has been presented as a thyristor binary switched capacitor (TBSC) bank and thyristor binary switched reactor (TBSR) bank in a cascade closed-loop operation as fine and coarse control actions. These capacitors and reactors are made switchable with the control law generated by the model reference adaptive controller is presented in this paper as a solution for dynamic variation in reactive power and voltage fluctuation in power systems and smart grid. TBSC-TBSR compensator is designed in a Matlab Simulink environment along with the dynamic load. While designing dynamic load, different loading conditions are considered steady-state load, sudden rise in load, sudden fall in load, and no-load condition as tracking conditions. Then the system identification toolbox is used to find out the appropriate plant model and load model transfer function. Further, the plant and load model transfer functions are used to design model reference adaptive controller (MRAC). To design, MRAC needs a reference model. To enhance the system performance, three different reference models are considered as under, over, and critically damped. Here, the TBSC-TBSR compensator with MRAC is used to suppress the dynamic variation in load to improve performance specifications of the compensator in the form of rise time, settling time, and peak overshoot along with different adaptation gains (γ) with different damping conditions.

Desirable features:

1. Adaption of system performance is taking place. At every new occurrence of load disturbance,

controller parameters get adjusted to a new value until they reach to steady-state condition.

2. It improves system performance t_r , t_s , and m_p continuously at every new occurrence of load disturbance until it settles to new steady-state values of controller parameters.
3. It gives good results for fast dynamic load variations.
4. It is applicable for linear and nonlinear loads also.

2. Proposed topology

In any electrical system, reactive power compensation plays an important role in controlling voltage profile and maintaining voltage stability. To achieve this, it requires fast compensating devices. These fast compensating devices are considered in two parts, one dynamic and the second static. The dynamic compensator has been dealt with thyristor binary switched capacitor (TBSC) while static compensator is dealt with thyristor binary switched capacitor and thyristor binary switched reactor (TBSR) as a fine-tuning. Let us consider an example of an end-user with a distribution system having a mixed load. The compensating scheme proposed for this is with four capacitor banks and four reactor banks.

The proposed scheme shown in Figure 2 consists of a capacitor and reactor banks with thyristor as a switch, which is connected in shunt with load at the point of common coupling (PCC). The controller gives the switching signals to the thyristors based on the reactive power demand of the load to switch ON and OFF

capacitor and reactor banks. TSC and TSR banks are arranged in binary-weighted sequential steps known as TBSC and TBSR.

and their values are obtained as follows:

$$Q_{TBSC} = 2^3 Q_C + 2^2 Q_C + 2^1 Q_C + 2^0 Q_C$$

$$Q_{TBSR} = 8 Q_C + 4 Q_C + 2 Q_C + 1 Q_C \quad (1)$$

2.1. Structure of The TBSC compensator

Assume the Q_{TBSC} is the maximum reactive power to be compensated and minimum step size allotted is of Q_C , then with four stepped switched capacitor banks

Where,

Q_{TBSC} = Total reactive power of the capacitor bank.

Q_C = reactive power of smallest capacitor.

If the smallest step value of capacitor bank is assumed to be $Q_C = 1KVA_r$ then, the total maximum

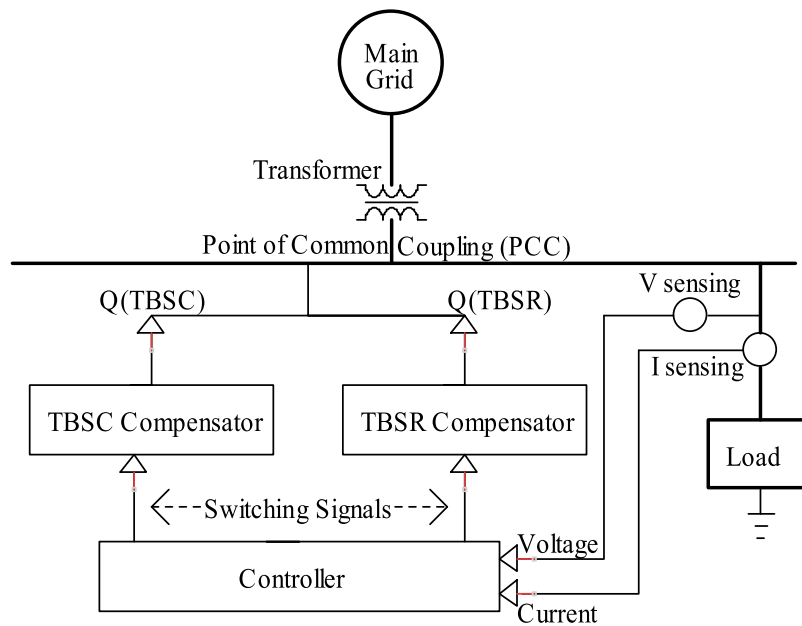


Figure 2. Proposed topology.

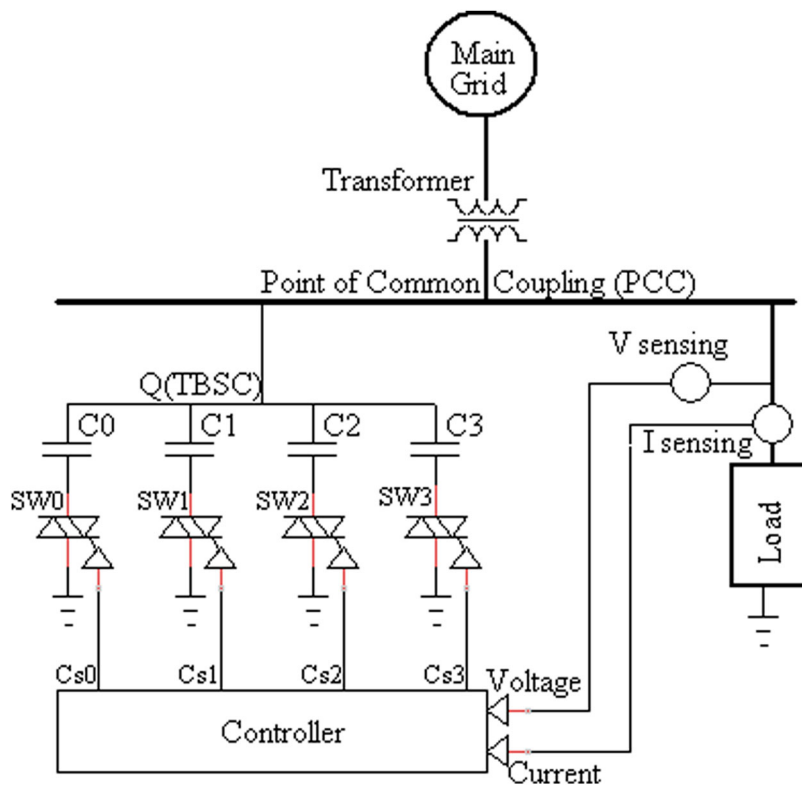


Figure 3. Thyristor binary connected capacitor bank.

compensation is given by;

$$Q_{TBSC} = 8 * 1000 + 4 * 1000 + 2 * 1000 + 1 * 1000$$

Then the subsequent binary steps will be as follows;

$$\text{The binary step [0001] lowest} = Q_C = 1KVAR \quad (2)$$

$$\text{The binary step [0010]} = 2Q_C = 2KVAR \quad (3)$$

$$\text{The binary step [0100]} = 4Q_C = 4KVAR \quad (4)$$

$$\text{The binary step [1000]} = 8Q_C = 8KVAR \quad (5)$$

All the above capacitor banks used are 3 phase 4 wire star connected systems and switched IN and OUT with a thyristor as a solid-state relay. The entire scheme is shown in Figure 3 schematically.

The four capacitors C0, C1, C2, and C3 have a magnitude in the range of 8421 code. This arrangement gives 2^4 switching states as given by Equations 1–5. The general technical datasheets give the information that capacitors have a 2% loss based on the loss angle of the capacitor. Using this technical information, the details regarding these capacitors are chosen as given in Table 1.

2.2. Structure of The TBSR compensator

From basic equations (2, 3, 4, and 5), the switching pattern of the capacitor bank is binary stepped with the lowest step $Q_C = 1KVAR$. There are 16 switched states. The lowest value of compensation is $Q_C = 1KVAR$. It is the lowest resolution of this scheme. Therefore, whatever compensation is required in between 0 to $1KVAR$,

Table 1. The technical details of capacitor bank assumption for Matlab simulation.

Sr. No.	Total VAR output	The value of the capacitor (C) in μf	2% loss of capacitor in ohm	Reactance of capacitor in ohm
1	$1Q_C = 1000$	$C_0 = 19.90$	00.32	160.00
2	$2Q_C = 2000$	$C_1 = 39.81$	00.16	80.00
3	$4Q_C = 4000$	$C_2 = 79.62$	00.08	40.00
4	$8Q_C = 8000$	$C_3 = 159.24$	00.04	20.00

it remains as $1KVAR$ leading error. Then, this error of overcompensation (0 to $1KVAR$) is further nullified by fine-tuning arrangements made by once again thyristor binary switched reactor bank (TBSR), showing in Figure 4.

The four inductors L0, L1, L2, and L3, are connected in parallel with the TBSC bank, and their magnitude and switching arrangement are made once again binary switching pattern. The error in compensation by TBSC bank in the value of the lowest bank or $1KVAR$ assumed in this case. This $1KVAR$ error has been divided once again by four reactor banks, as shown in Figure 4. In this case, also switching states becomes a 16. The resolution of compensation becomes $\frac{1}{2^4}$.

The total compensation done by the reactors will be as follows:

$$Q_{TBSR} = 2^3 Q_L + 2^2 Q_L + 2^1 Q_L + 2^0 Q_L$$

$$Q_{TBSR} = 8Q_L + 4Q_L + 2Q_L + 1Q_L \quad (6)$$

Where,

Q_{TBSR} is the total reactive power of the TBSR compensator, and Q_L is its lowest step value of lagging

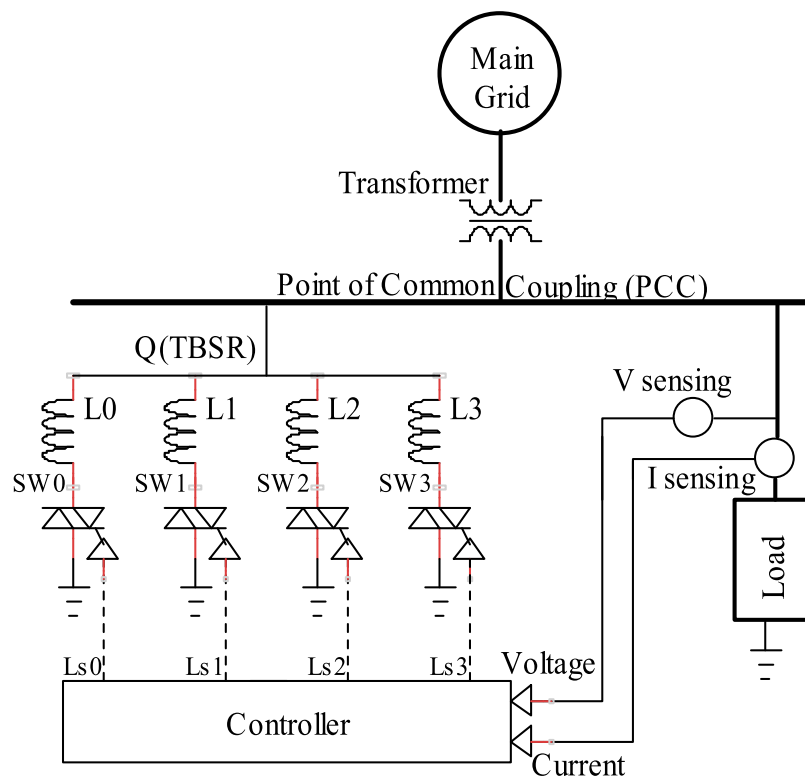


Figure 4. Thyristor binary connected reactor bank for fine-tune arrangement.

Table 2. The technical details of reactor bank assumption for Matlab simulation.

Sr. No.	Q_{TBSR} in VAR	The inductor value used in Henry	Inductive reactance (X_L) in ohm
1	$1Q_L = 62.5$	$L_0 = 5.09$	1600
2	$2Q_L = 125$	$L_1 = 2.55$	800
3	$4Q_L = 250$	$L_2 = 1.27$	400
4	$8Q_L = 500$	$L_3 = 0.32$	200

power. The smallest step value of the reactor bank is selected as $Q_L = 62.5VAR$.

$$Q_{TBSR} = 8 * 62.5 + 4 * 62.5 + 2 * 62.5 + 1 * 62.5$$

$$Q_{TBSR} = 1000VAR \quad (7)$$

The subsequent binary steps for their combination will be the same as capacitor banks, but the magnitude will be 62.5, 125, 250, and 500 VAR's are specified in Table 2. These reactor banks are 3 phase, 4 wire systems with star connected. This TBSR fine-tuned compensator scheme has been shown in Figure 4.

3. Overall binary switching arrangement of capacitor and reactor bank

From Figure 2, it is observed that the corresponding capacitor and reactor banks which are arranged in their binary values are connected in the shunt. The overcompensation taken place by the capacitor bank is taken care of by the reactor bank. Both these capacitor and reactor banks are in cascaded form. The error due to capacitor bank (TBSC) will act as a set point to reactor bank (TBSR). This closed-loop arrangement is shown in Figure 7.

3.1. The feedback configuration system of VAR generator

The overall capacitor switching arrangement in the closed-loop is shown in Figure 5, and their linkage is as given below.

Setpoint: this signal is the set point for which this configuration works irrespective of load side reactive power demand. This will give the setpoint value of reactive power with load-side disturbance rejection.

Load disturbance (Q_L): The reactive power demand of the load to be compensated is evaluated by measuring load side voltage, current, and phase angle between them. The feedback signal will be reactive load disturbance (Q_L) + leading reactive power supplied by the capacitor bank (Q_{TBSC}). By comparing this signal with the setpoint, the error signal becomes $Error = Q_{ref} - (Q_{TBSC} - Q_{Load})$.

4 bit ADC block: The four capacitor banks are to be switched in or out. These switching signals are generated by a 4 bit ADC. The error signal is ultimately

converted into switching pulse width modulation signal as C_{S0} , C_{S1} , C_{S2} , and C_{S3} .

3.2. The feedback configuration system of VAR absorber

This closed-loop arrangement is the same as in the case of the switched capacitor bank. The overall compensation effect due to capacitor bank will be taken care of by reactor bank and operated in closed-loop control shown in Figure 6.

3.3. Cascade configuration system of VAR generator and absorber

The VAR generator and absorber are combined and connected in a cascade configuration, as shown in Figure 7. The capacitor switched configuration will act as a coarse controller, and switched reactor will act as a fine controller. This output of the coarse controller will serve as a set point to the fine controller. Their entire scheme of compensation was designed, build, and simulation results were tested by using Matlab. The entire system performance is evaluated based upon the performance criterion t_r , t_s , and m_p . These system performance parameters can be improved by upgrading the adaptation gain and reference model. To upgrade the performance parameters model reference adaptive controller (MRAC) has been designed, and simulated results were obtained in the subsequent section.

4. Model Reference Adaptive Controller (MRAC)

From the design of TBSC and TBSR, it is identified that the parameters such as voltage and frequency vary, the compensation goes on changing. Also, capacitors and reactors are get affected by aging effects. In such a variable parameter environment, conventional tuned PID will not be sufficient. There must be a sum mechanism that will vary the PID tuning parameters. In such a situation, adaptive controllers play an important role in handling unknown parameter variations due to environmental changes, which leads to a nonlinear system. Also, sixteen possible ($2^N = 2^4 = 16$) switching states of the capacitor banks take place. Hence there are basically sixteen different transfer function appears at different situations which are difficult to control by fixed-gain controllers like PID. To cater this situation, a feedforward model reference adaptive controller structure is used and shown in Figure 8.

In this, controller parameters are adjusted by obtaining the error between plant output (Y_p) and reference model output (Y_m) as;

$$e = Y_p - Y_m \quad (8)$$

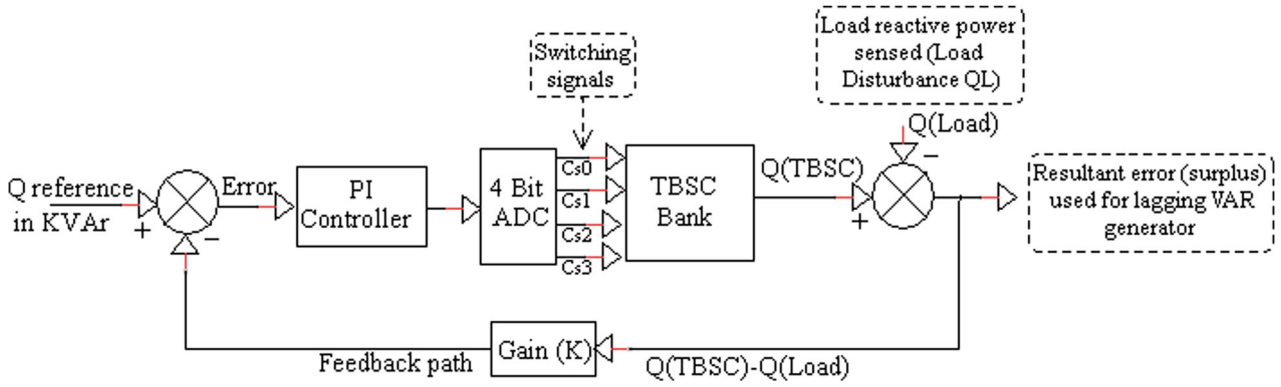


Figure 5. A feedback configuration system of VAR generator.

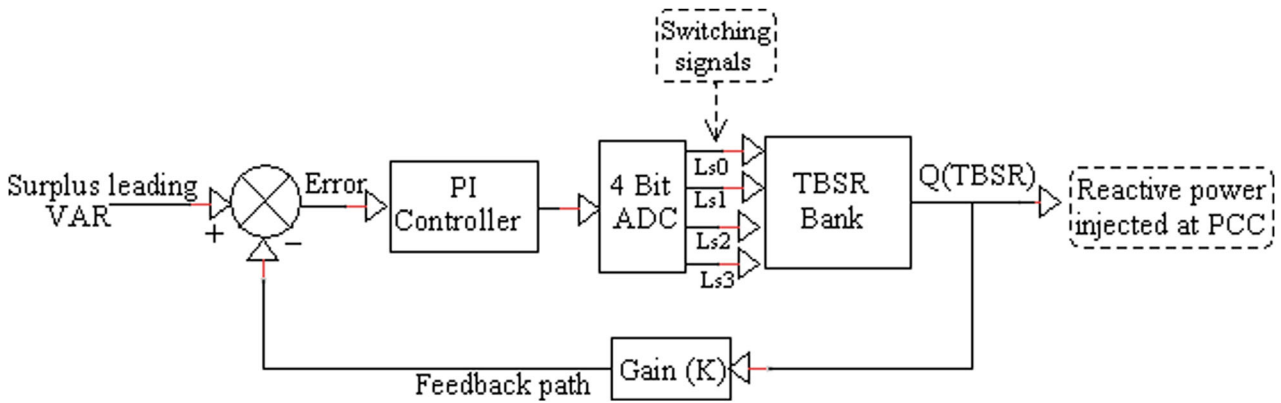


Figure 6. A feedback configuration system of VAR absorber.

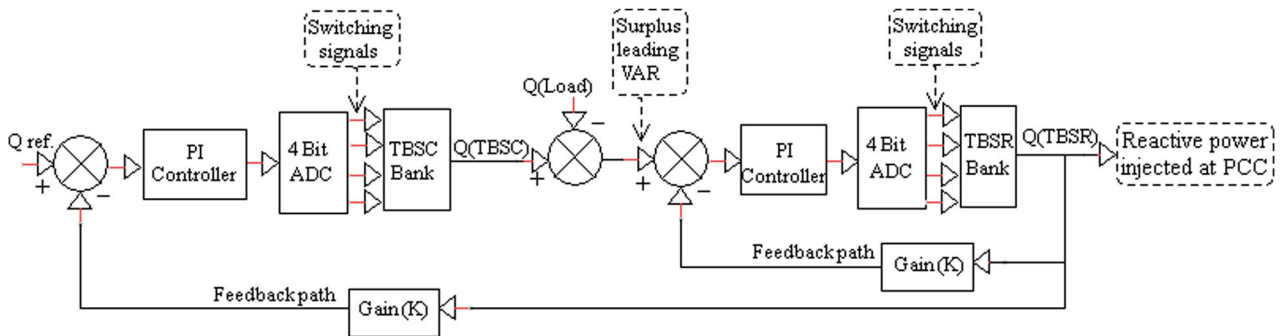


Figure 7. Cascade configuration system of VAR generator and absorber.

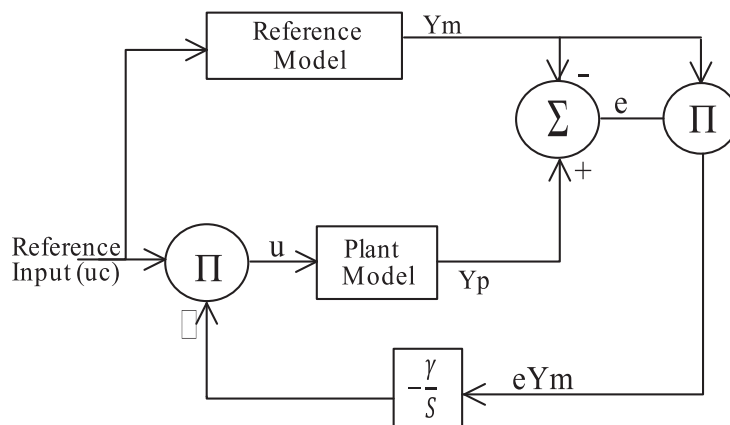


Figure 8. Feedforward mechanism of MRAC.

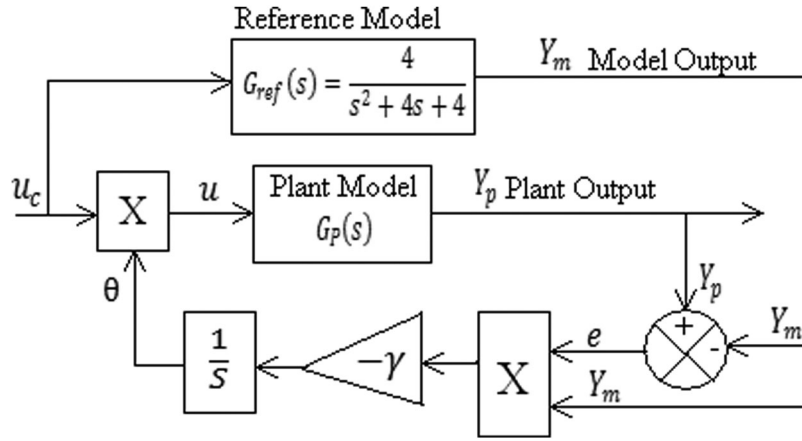


Figure 9. Overall MRAC controller structure.

As per MIT rule [39], cost function is defined as;

$$f(\theta) = \frac{e^2}{Z} \quad (9)$$

Where θ is known as the controller parameter, by MIT rule, this θ is adjusted such that cost function is minimized and the parameters variation direction should be negative.

The control equation for the plant input “u” is given by:

$u = u_c * \theta$; where u_c = reference input and θ is adjustment mechanism variable given by:

$$\theta = \int \gamma * Y_m * e \quad (10)$$

And, γ = variable gain.

$$\begin{aligned} \frac{d\theta}{dt} &= -\gamma e Y_m \text{ or } \theta = - \int \gamma e Y_m \text{ or } \theta(s) \\ &= \frac{-\gamma e(s) Y_m(s)}{s} \end{aligned} \quad (11)$$

These function has been represented in Figure 9.

As the system parameter varies, the control function also varies. It gets adjusted until the error between plant output Y_p and reference model output Y_m becomes zero, i.e. $e = Y_p - Y_m$. The response on TBSC, TBSR, and TBSC + TBSR will be governed by the nature of the reference model selected. These plants transfer functions are obtained using a system identification toolbox, and simulation results are obtained for critically, under, and over-damped reference models.

4.1. Plant model evaluation with system identification toolbox

With reference to section 3, the TBSC, TBSR, and combined TBSC-TBSR are designed, and performance has been evaluated by using Matlab Simulink. A complete Simulink diagram has been designed, and performance has been evaluated for transient free switching

of capacitor and reactor bank individually and combined [20–23]. The performance parameters such as t_r , t_s , and m_p are to be upgraded for fast compensation with a suitable controller. For the excellent performance of the plant, a good controller is required, which has been designed based on the mathematical model. It is difficult to obtain a mathematical model from the basic principles. To get the model, a system identification toolbox (SITB) has been utilized. Using this SITB from Matlab, a suitable transfer function with two poles and one zero has been determined as the numerator and denominator polynomial. The various test input signals such as step, ramp, pseudo-random binary signal, and impulse are used to generate the set of output data parameters. By storing these input-output data on workspace allows to visualize and analyze the data. These input-output relationships provide time constants, delay in response, and the number of poles and zeros. Hence knowing this information, the system transfer function is identified. The accuracy of the transfer function so determined is verified with the simulated data of the system, and the validation accuracy of the transfer function obtained is 99%.

The plant mathematical model in terms of transfer functions obtained are as follows:

- Thyristor binary switched Capacitor bank (TBSC), model.

$$G_c(s) = \frac{-0.002073 s + 1.018e^{-6}}{s^2 + 0.002442 s + 9.914e^{-7}} \quad (12)$$

It includes the blocks such as analog to digital converter (ADC), transient free switching logic generation, and thyristor switched binary capacitor bank.

- Thyristor binary switched Reactor bank (TBSR) model

$$G_r(s) = \frac{-0.03051 s + 1.389e^{-5}}{s^2 + 0.03944 s + 2.144e^{-5}} \quad (13)$$

It includes ADC, switching logic generation block and thyristor switched binary reactor bank.

- The mathematical model identified for the load disturbance model

$$G_l(s) = \frac{0.2523s + 0.0003131}{s^2 + 0.3782s + 0.003131} \quad (14)$$

This transfer function comes from the dynamic load block.

4.2. Selection of reference model

The block of MRAC implemented using MIT rule is shown in Figure 9. The second-order under the damped system is oscillatory in nature, giving more peaks and troughs. The output parameters of the compensator, which is reactive power or voltage goes on oscillating. If these oscillations are not damped out in a limited time period, then it may result in system instability. Therefore for ensuring stability, maximum overshoot/undershoot must be as low as possible. Ideally spiking, the response of system should be of step like in nature which has no transient. Therefore a reference model is selected having a critically damped second order system that has no oscillations and performance is somewhat similar to the first-order response. Hence basic reference model is taken as;

With critically damping factor ($\zeta = 1$).

$$G_{ref}(s) = \frac{4}{(s^2 + 4s + 4)} \quad (15)$$

For experimentation and comparison purposes other two reference models selected are with underdamped ($\zeta < 1$) and overdamped ($\zeta > 1$) are as follows; With underdamped factor ($\zeta = 0.35$).

$$G_{ref}(s) = \frac{0.2025}{(s^2 + 1.625s + 0.2025)} \quad (16)$$

With over-damped factor ($\zeta = 1.8$).

$$G_{ref}(s) = \frac{0.2025}{(s^2 + 0.315s + 0.2025)} \quad (17)$$

With natural frequencies of oscillation as $\omega_n = 2, 0.45$ and 0.45 rad/sec. respectively.

5. Responses of the compensators TBSC, TBSR, and TBSC + TBSR, with MRAC

As mentioned above, simulations are carried out for TBSC, TBSR, and TBSC + TBSR with different reference models. For all these simulations, a reference input has been used as a step input. The step input function is one of the conventional standard test signals. Conventionally steady-state errors are calculated by providing an input function, which goes to zero as the time approaches infinity theoretically. Here we can find out

Table 3. The performance parameter of TBSC for critically damped reference model.

Model used	Gamma Selected	t_r in sec	t_s in sec	m_p in %
TBSC	50	2.8	4.5	0.0

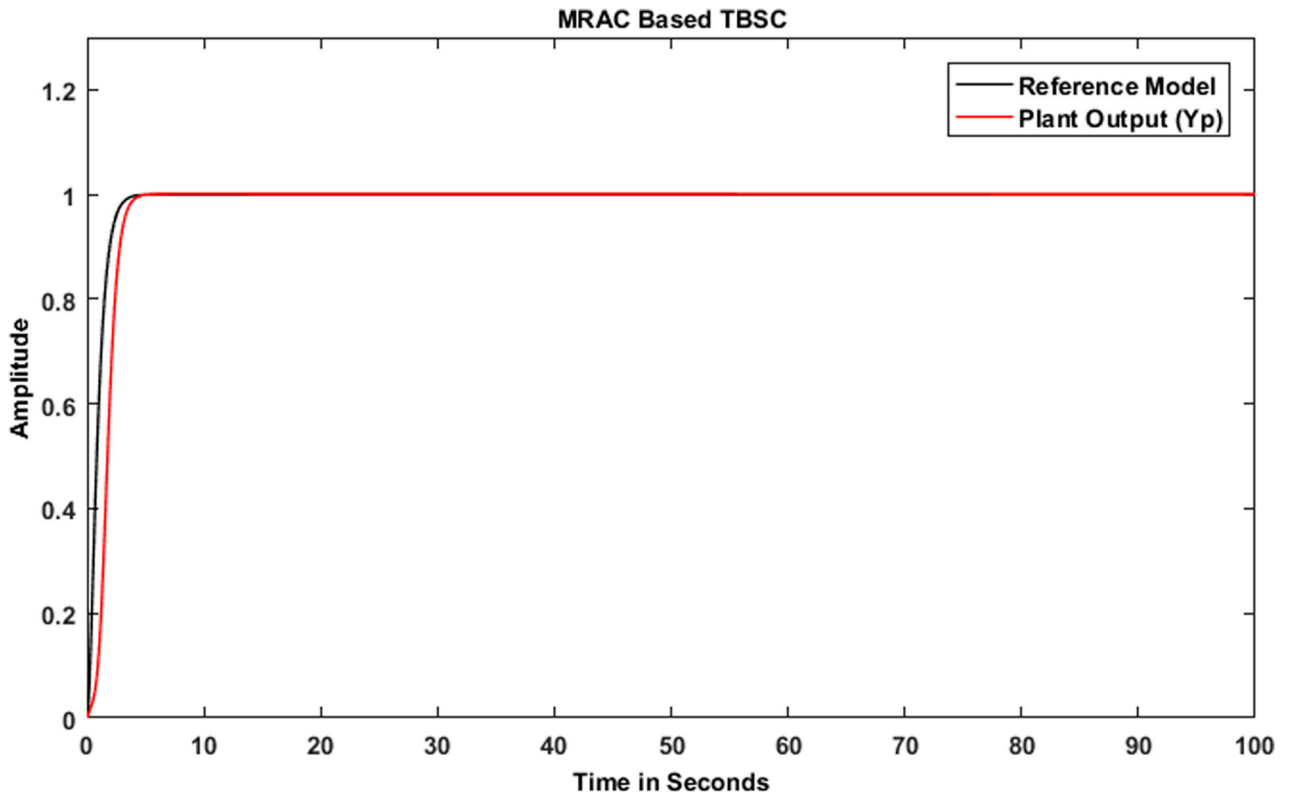


Figure 10. The response of TBSC with MRAC having critically damped reference model.

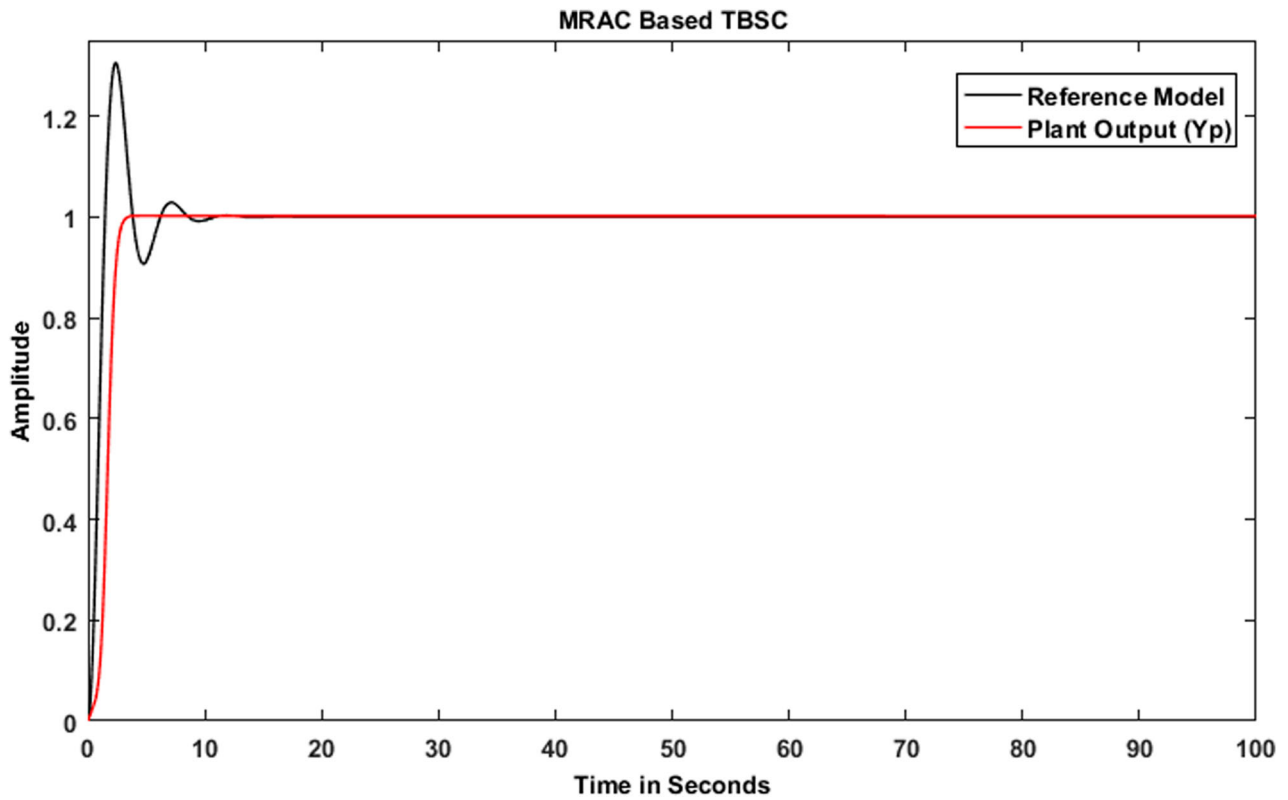


Figure 11. The response of TBSC with MRAC having under a critically damped reference model.

Table 4. The performance parameter of TBSC for underdamped reference model.

Model used	Gamma Selected	t_r in sec	t_s in sec	m_p in %
TBSC	50	2.4	3.5	0.0

Table 5. The performance parameter of TBSC for overdamped reference model.

Model used	Gamma Selected	t_r in sec	t_s in sec	m_p in %
TBSC	50	17.48	84	0.0

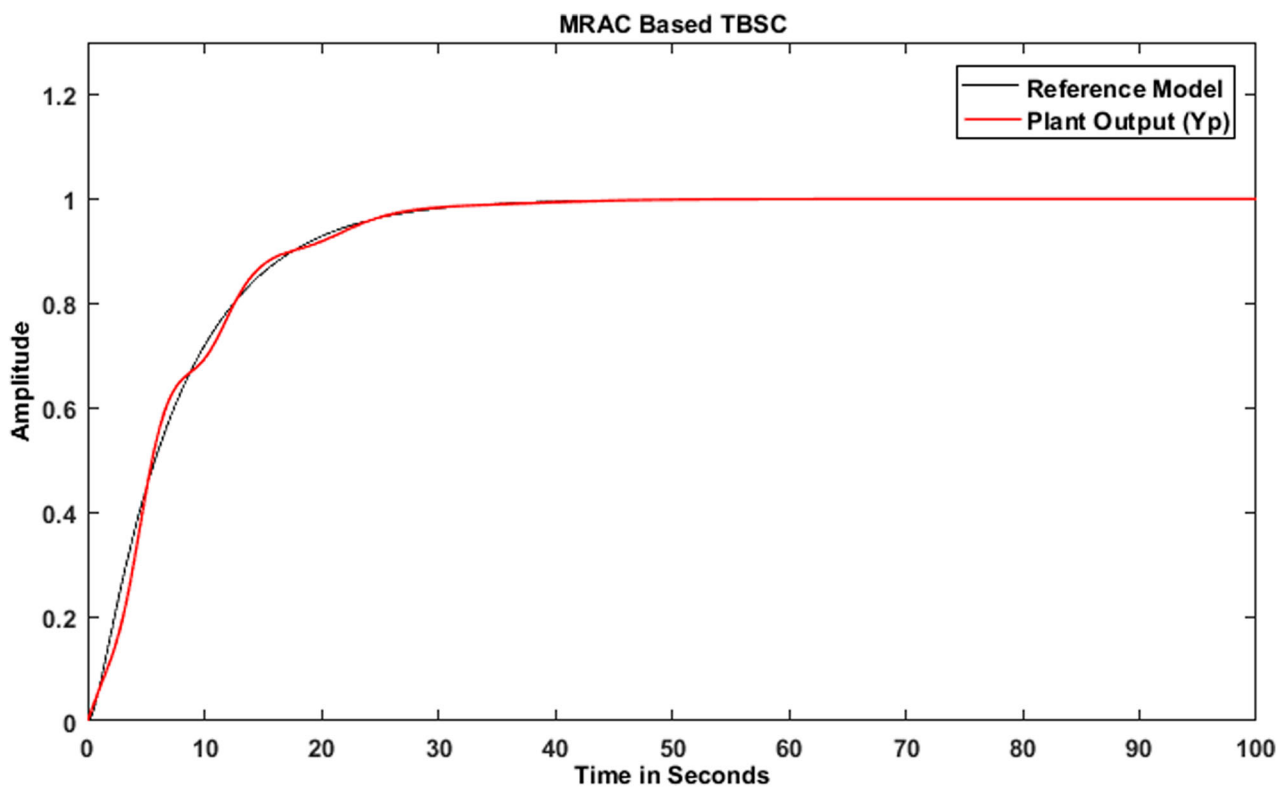


Figure 12. The response of TBSC with MRAC having overdamped reference model.

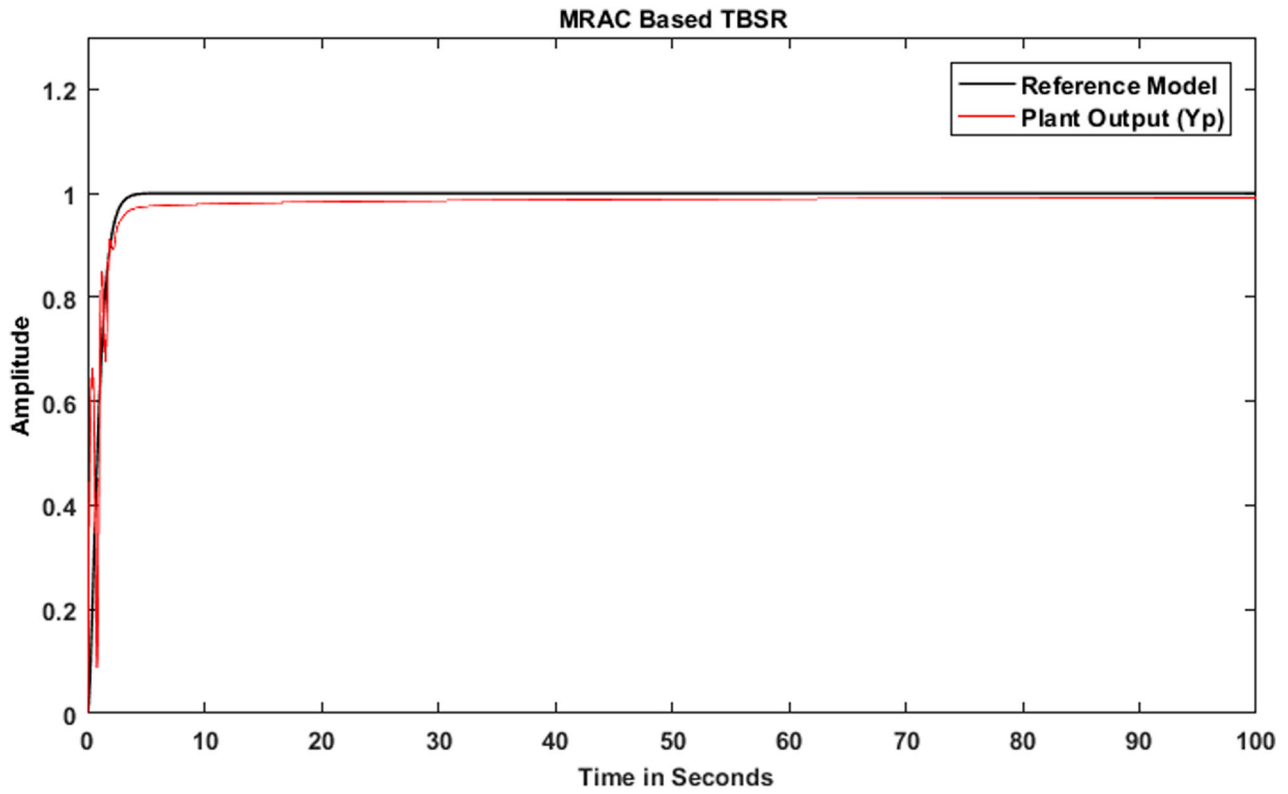


Figure 13. The response of TBSR with MRAC having critically damped reference model.

Table 6. The performance parameter of TBSR for critically damped reference model.

Model used	Gamma Selected	t_r in sec	t_s in sec	m_p in %
TBSR	50	1.86	100	0.0

Table 7. The performance parameter of TBSC for underdamped reference model.

Model used	Gamma Selected	t_r in sec	t_s in sec	m_p in %
TBSR	50	1.19	100	14%

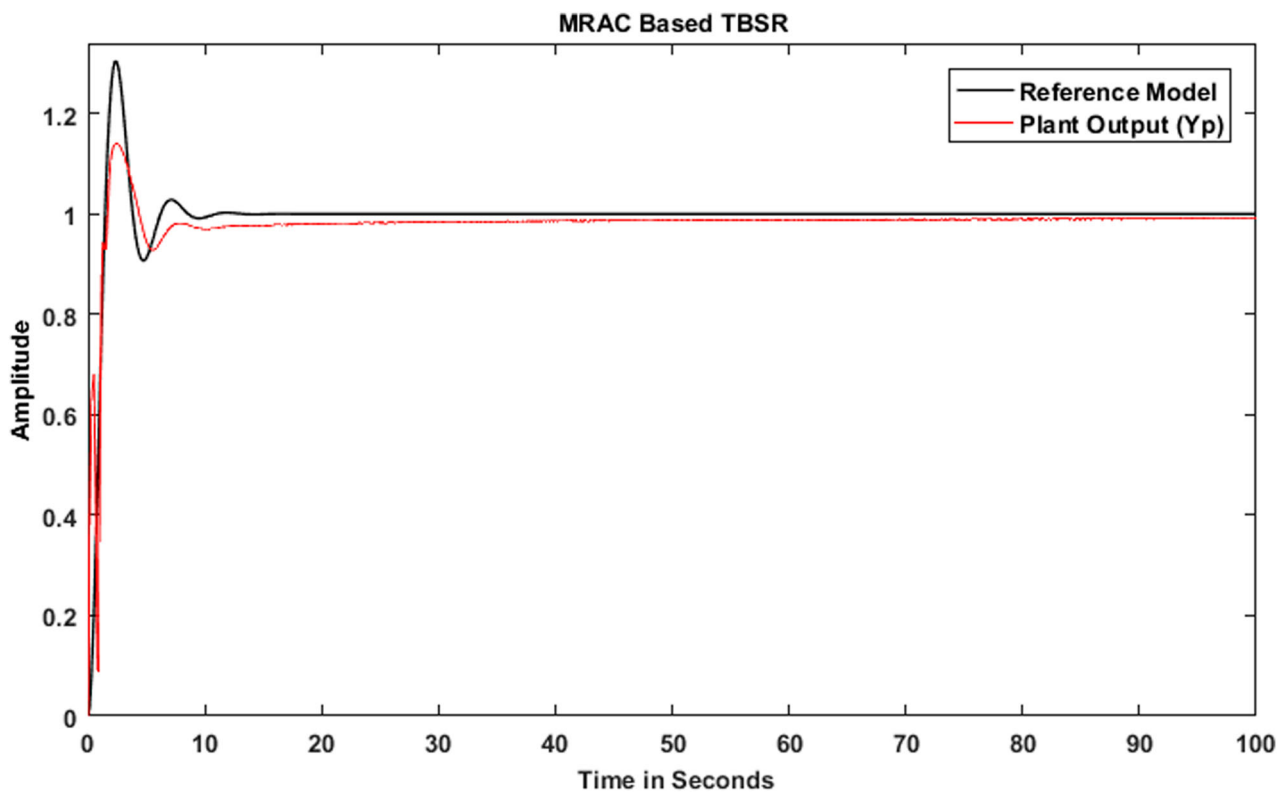


Figure 14. The response of TBSR with MRAC having underdamped reference model.

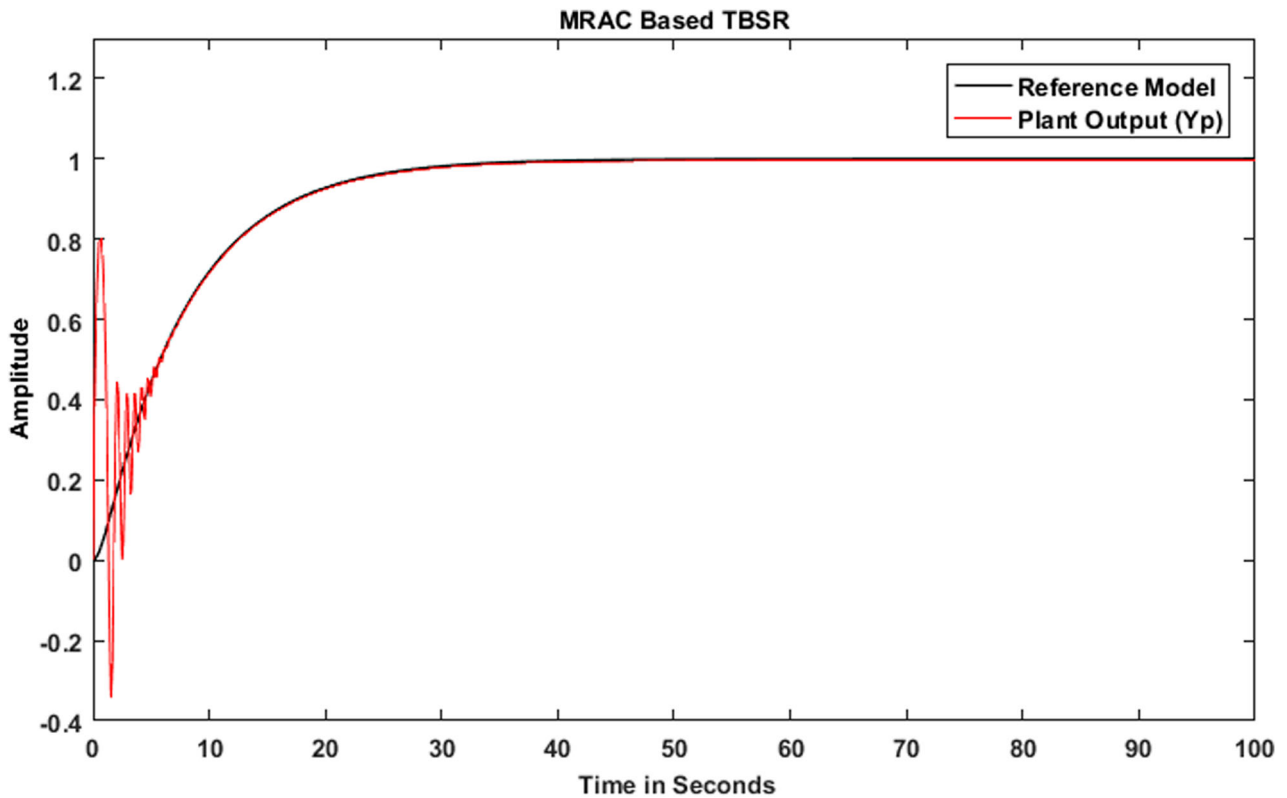


Figure 15. The response of TBSR with MRAC having overdamped reference model.

Table 8. The performance parameter of TBSR for overdamped reference model.

Model used	Gamma Selected	t_r in sec	t_s in sec	m_p in %
TBSR	50	17.84	60	0.0

Table 9. The performance parameter of TBSC + TBSR for critically damped reference model.

Model used	Gamma Selected	t_r in sec	t_s in sec	m_p in %
TBSC + TBSR	50	2.6	21.16	0.0

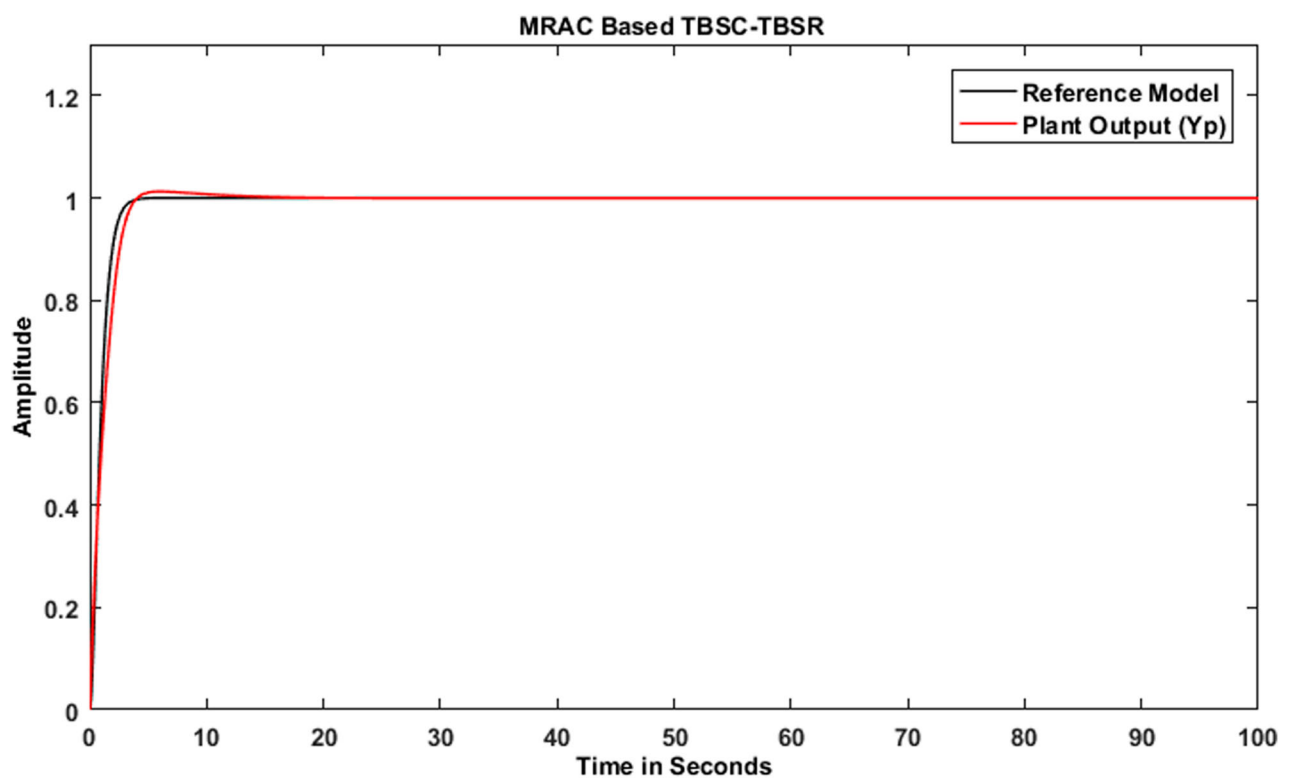


Figure 16. The response of TBSC-TBSR with MRAC having critically damped reference model.

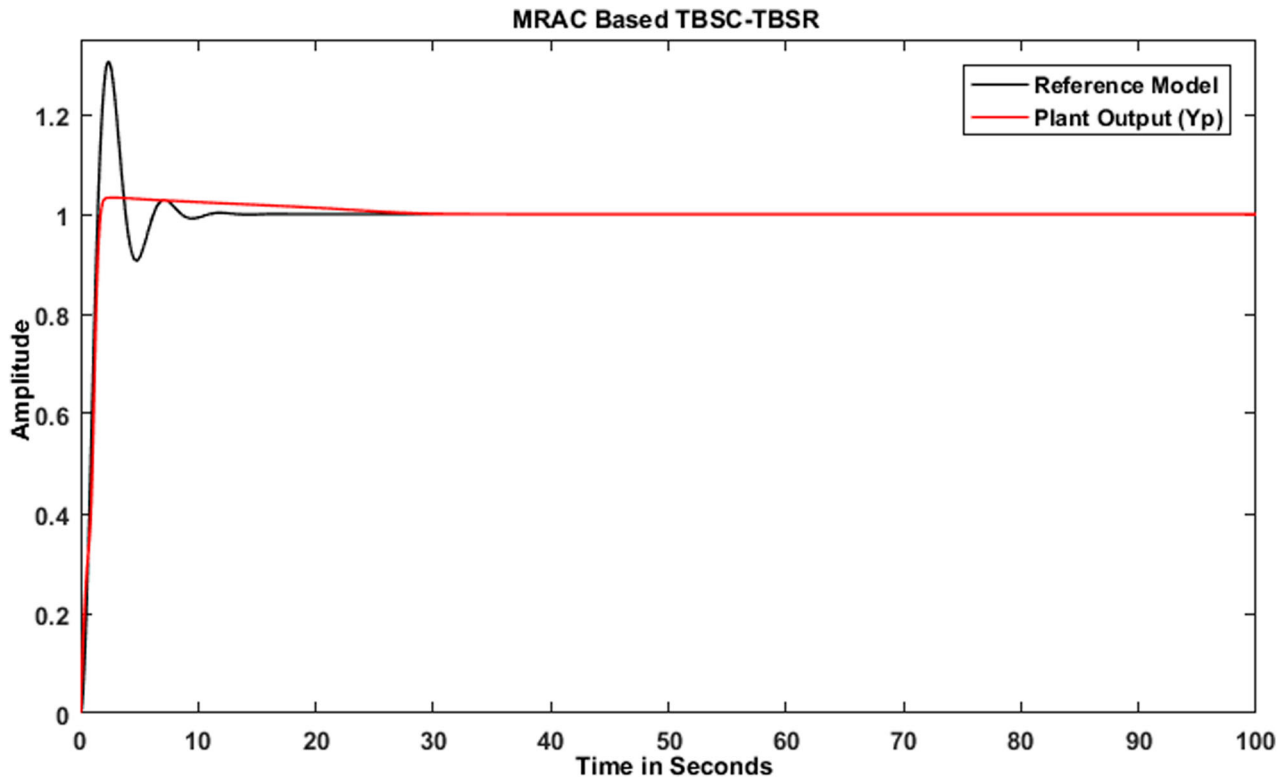


Figure 17. The response of TBSC-TBSR with MRAC having underdamped reference model.

Table 10. The performance parameter of TBSC + TBSR for underdamped reference model.

Model used	Gamma Selected	t_r in sec	t_s in sec	m_p in %
TBSC + TBSR	50	1.588	39.86	0.0

Table 11. The performance parameter of TBSC + TBSR for overdamped reference model.

Model used	Gamma Selected	t_r in sec	t_s in sec	m_p in %
TBSC + TBSR	50	14.53	86.5	0.0

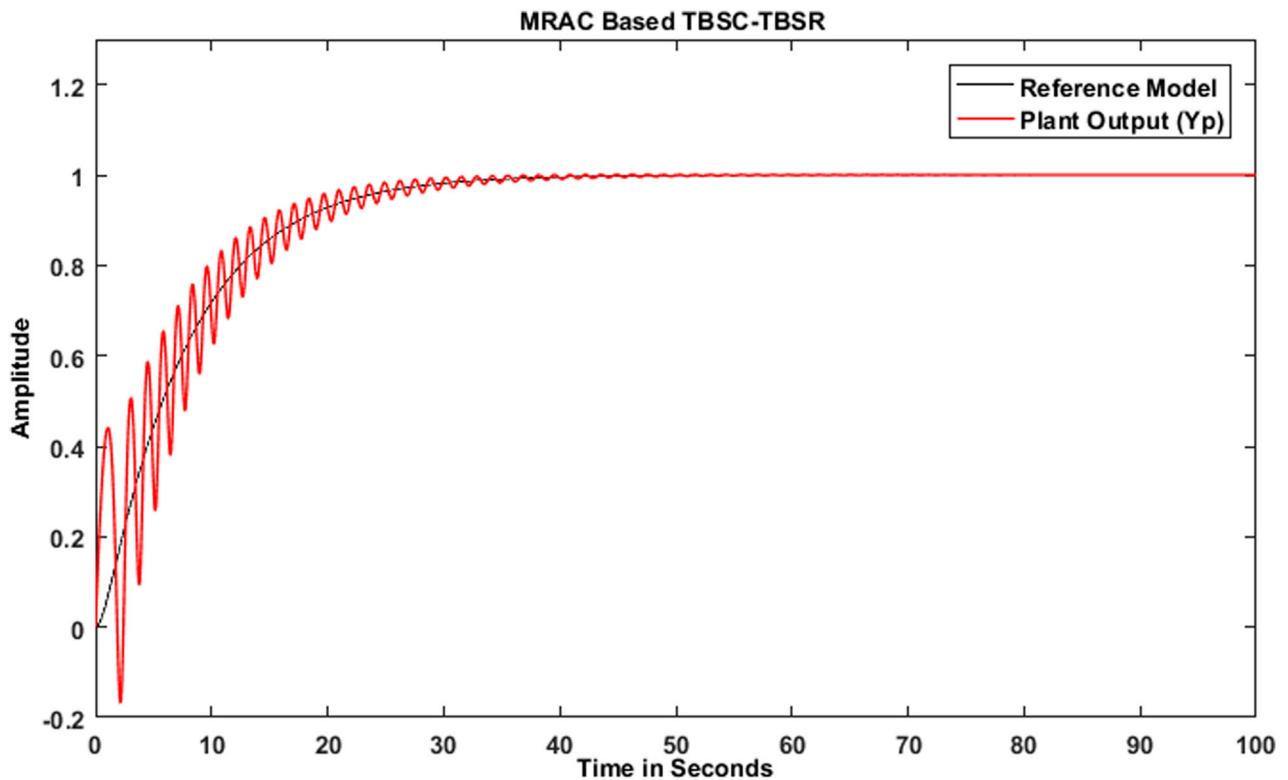


Figure 18. The response of TBSC-TBSR with MRAC having overdamped reference model.

Table 12. Results of MRAC based TBSC for different values of gamma.

Gamma (γ)	t_r , t_s and m_p in sec	Critically damped	Under damped	Over damped
$\gamma = 0$	tr (sec)	33.85	33.66	33.66
	ts (sec)	> 200	> 200	> 200
	mp (%)	0	0	0
$\gamma = 0.1$	tr (sec)	21.47	20.5	28.9
	ts (sec)	> 100	60	> 100
	mp (%)	0	0	0
$\gamma = 0.5$	tr (sec)	12.18	11.00	21.98
	ts (sec)	28	25	50
	mp (%)	0	0	0
$\gamma = 1$	tr (sec)	9.07	7.8	18.9
	ts (sec)	20	18	60
	mp (%)	0	0	0
$\gamma = 5$	tr (sec)	4.5	3.4	13.8
	ts (sec)	10	8	60
	mp (%)	0	0	0
$\gamma = 10$	tr (sec)	3.3	2.4	14
	ts (sec)	8	6	50
	mp (%)	0	0	0
$\gamma = 20$	tr (sec)	2.6	1.9	16.63
	ts (sec)	6	4.5	50
	mp (%)	0	0	0
$\gamma = 50$	tr (sec)	2.8	2.4	17.48
	ts (sec)	4.5	3.45	84
	mp (%)	0	0	0
$\gamma = 100$	tr (sec)	2.5	2.17	14.9
	ts(sec)	4	2.8	40
	mp (%)	0	0	0

Table 13. Results of MRAC based TBSR for different values of gamma.

Gamma	t_r , t_s and m_p in sec	Critically damped	Under damped	Over damped
$\gamma = 0$	tr (sec)	0.40	0.40	0.41
	ts (sec)	> 200	> 200	> 200
	mp (%)	0	0	0
$\gamma = 0.1$	tr (sec)	0.439	0.439	0.437
	ts (sec)	> 200	> 200	> 200
	mp (%)	0	0	0
$\gamma = 0.5$	tr (sec)	27.05	26.74	31.4
	ts (sec)	> 200	> 200	> 200
	mp (%)	0	0	0
$\gamma = 1$	tr (sec)	17.35	17.121	24.41
	ts (sec)	> 200	> 200	> 200
	mp (%)	0	0	0
$\gamma = 5$	tr (sec)	4.84	1.94	18.44
	ts (sec)	> 200	> 200	> 200
	mp (%)	0	0	0
$\gamma = 10$	tr (sec)	3.01	1.6	17.72
	ts (sec)	> 200	> 200	> 200
	mp (%)	0	4.5	0
$\gamma = 20$	tr (sec)	2.4	1.42	15.12
	ts (sec)	> 200	> 200	> 200
	mp (%)	0	9	0
$\gamma = 50$	tr (sec)	1.86	1.192	17.84
	ts (sec)	> 200	> 200	60
	mp (%)	0	14	0
$\gamma = 100$	tr (sec)	1.17	0.594	14.34
	ts(sec)	160	160	45
	mp (%)	0	17.3	0

the system response parameter such as t_r , t_s , and m_p . These time response specifications are obtained where input changes suddenly from zero to one and then one to zero. Applying repeated such sequence, it becomes the square wave input. In adaptive control systems, the plant performance must track the reference input in accordance with the reference model. This will be a representation of sudden load disturbance demand.

5.1. Response of TBSC compensator

5.1.1. Reference model with critically damped ($\zeta = 1$)

The plot is shown in Figure 10. It is a plot of reference model output and plant model output v/s time. The different performance parameters are shown in Table 3.

Table 14. Results of MRAC based TBSC-TBSR for different values of gamma.

Gamma	t_r , t_s and m_p in sec	Critically damped	Under damped	Over damped
$\gamma = 0$	t_r (sec)	2.66	3.06	3.061
	t_s (sec)	10	10	10
	m_p (%)	0	0	0
$\gamma = 0.1$	t_r (sec)	3.04	2.984	3.02
	t_s (sec)	10	8	> 80
	m_p (%)	0	0	0
$\gamma = 0.5$	t_r (sec)	2.96	2.66	3.2
	t_s (sec)	7	5	40
	m_p (%)	0	0	0
$\gamma = 1$	t_r (sec)	2.87	2.5	3.5
	t_s (sec)	6	30	40
	m_p (%)	0	1.4	0
$\gamma = 5$	t_r (sec)	2.4	2.03	7.5
	t_s (sec)	15	30	50
	m_p (%)	1.2	2.9	0
$\gamma = 10$	t_r (sec)	2.18	1.8	5.83
	t_s (sec)	12	30	60
	m_p (%)	1.4	3.2	0
$\gamma = 20$	t_r (sec)	1.9	1.6	9.4
	t_s (sec)	8	30	60
	m_p (%)	1.2	3.3	0
$\gamma = 50$	t_r (sec)	2.56	1.58	14.42
	t_s (sec)	21.16	39.86	86.5
	m_p (%)	0	3.3	0
$\gamma = 100$	t_r (sec)	1.6	1.3	13.14
	t_s (sec)	4	28	50
	m_p (%)	0	3.3	0

5.1.2. Reference model with underdamped ($\zeta = 0.35$)

The plot is shown in Figure 11, and the different performance parameters are shown in Table 4.

5.1.3. Reference model with over-damped

The plot is shown in Figure 12, and the different performance parameters are shown in Table 5.

5.2. Response of TBSR compensator with MRAC

The response of the thyristor binary switched reactor is obtained with MRAC having different reference models, as used in TBSC and listed as below:

5.2.1. Reference model with critically damped

The plot of plant output Y_p and reference model Y_m is shown in Figure 13. The different performance parameters are listed in Table 6.

5.2.2. Reference model with underdamped

Plant and reference model output parameters Y_p and Y_m are plotted in Figure 14. The different performance parameters are listed in Table 7.

5.2.3. Reference model with overdamped

Plant and reference model output parameters Y_p and Y_m are plotted in Figure 15. The different performance parameters are listed in Table 8.

The different performance parameters are listed in Table 8.

5.3. Response of TBSC + TBSR compensator with MRAC

In this case, TBSC and TBSR are cascaded together with MRAC, and results are obtained for different reference models as previously done.

5.3.1. Reference model with critically damped

Plant output Y_p and reference model output Y_m are shown in Figure 16. The different performance parameters are listed in Table 9.

5.3.2. Reference model with underdamped

Plant output Y_p and reference model output Y_m are shown in Figure 17. The different performance parameters are listed in Table 10.

5.3.3. Reference model with overdamped

Plant output Y_p and reference model output Y_m are shown in Figure 18. The different performance parameters are listed in Table 11.

6. Response of the plant for different values of adaptation gain gamma (γ)

From equations 10 and 11, it is found that the performance of the plant is influenced by the adaptation gain gamma. For different values of gamma, the performance of MRAC based VAR compensator (TBSC, TBSR, and TBSC-TBSR) for the three different reference models are shown in Tables 12–14.

It is observed from Tables 12–14 that, as the value of adaptation gain gamma increases from 0 to 100, the system response gets improved.

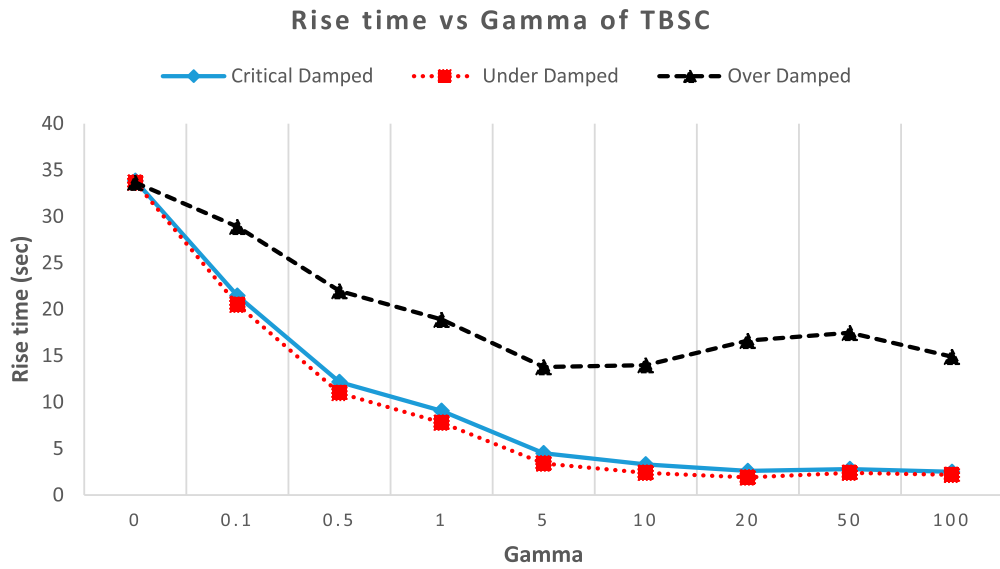


Figure 19. Comparison of MRAC TBSC for different values of gamma with rise time.

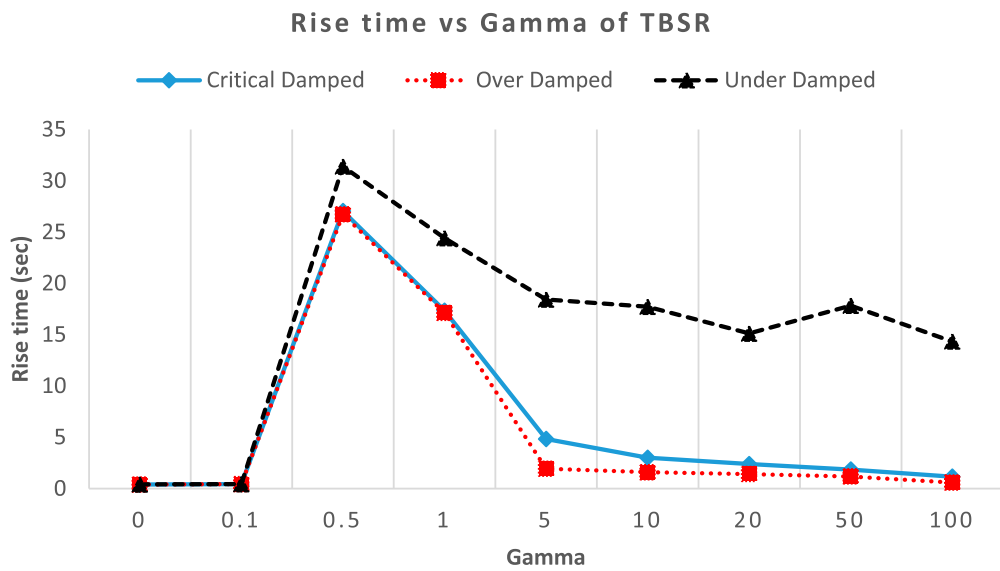


Figure 20. Comparison of MRAC TBSR for different values of gamma with rise time.

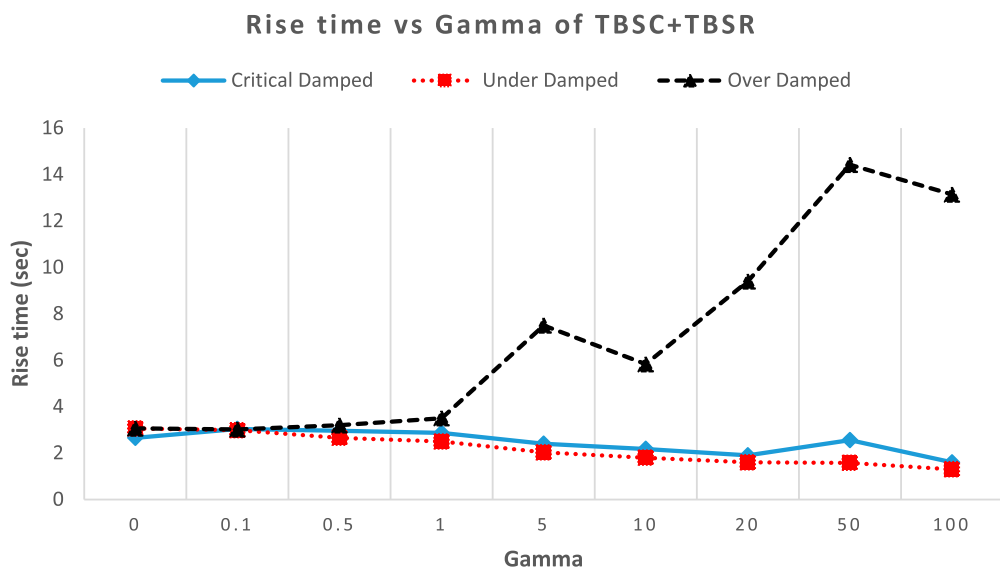


Figure 21. Comparison of MRAC TBSC + TBSR for different values of gamma with rise time.

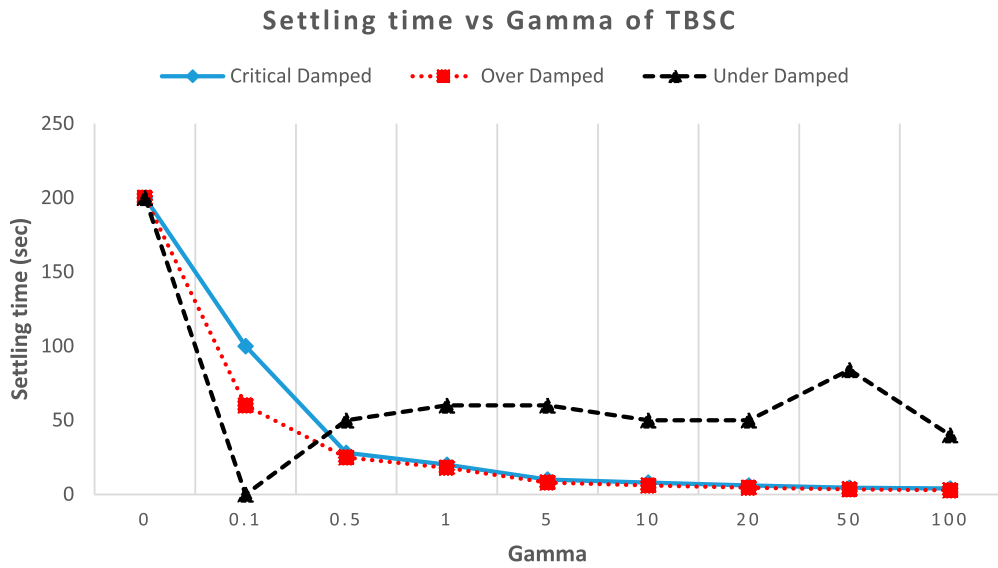


Figure 22. Comparison of MRAC TBSC for different values of gamma with settling time.

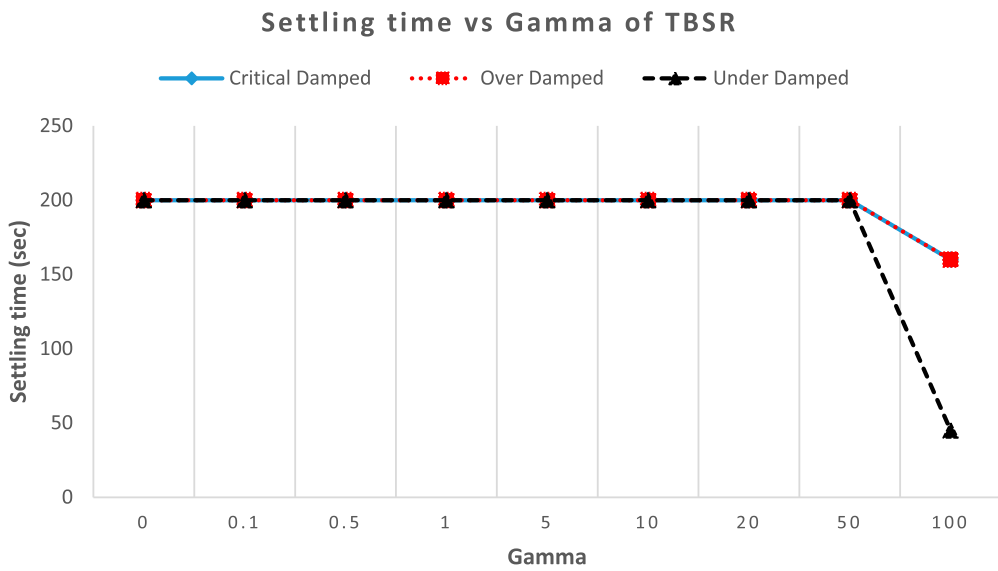


Figure 23. Comparison of MRAC TBSR for different values of gamma with settling time.

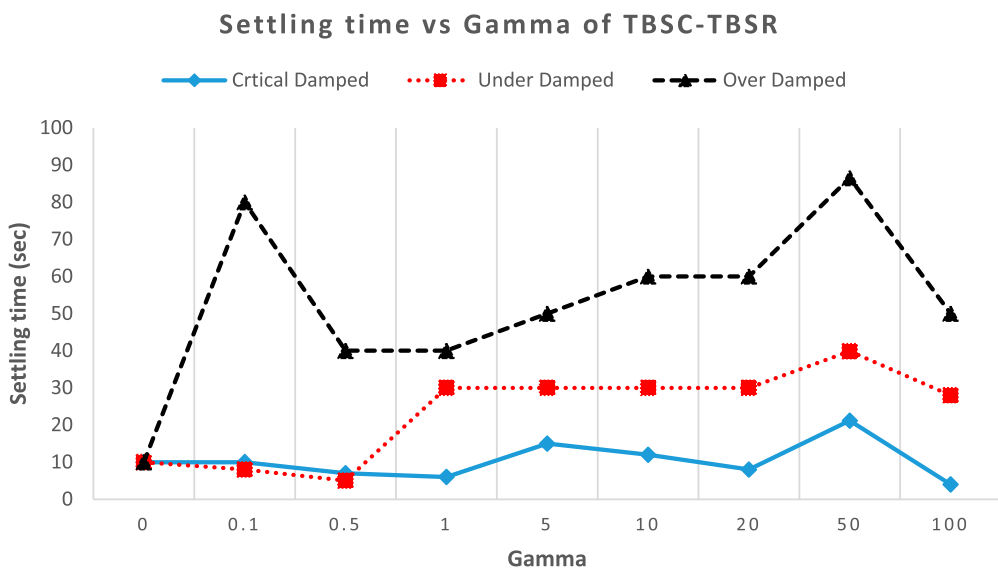


Figure 24. Comparison of MRAC TBSC-TBSR for different values of gamma with settling time.

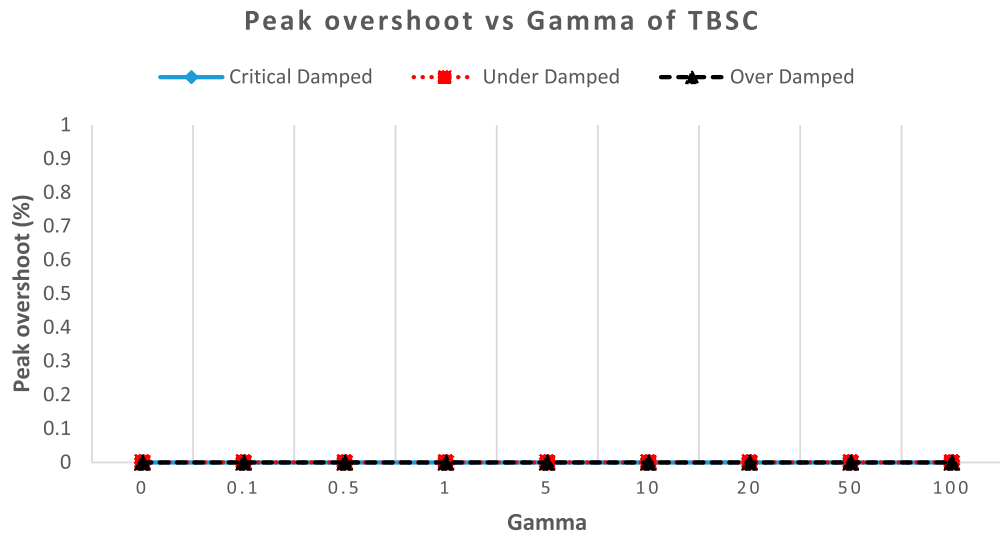


Figure 25. Comparison of MRAC TBSC for different values of gamma with peak overshoot.

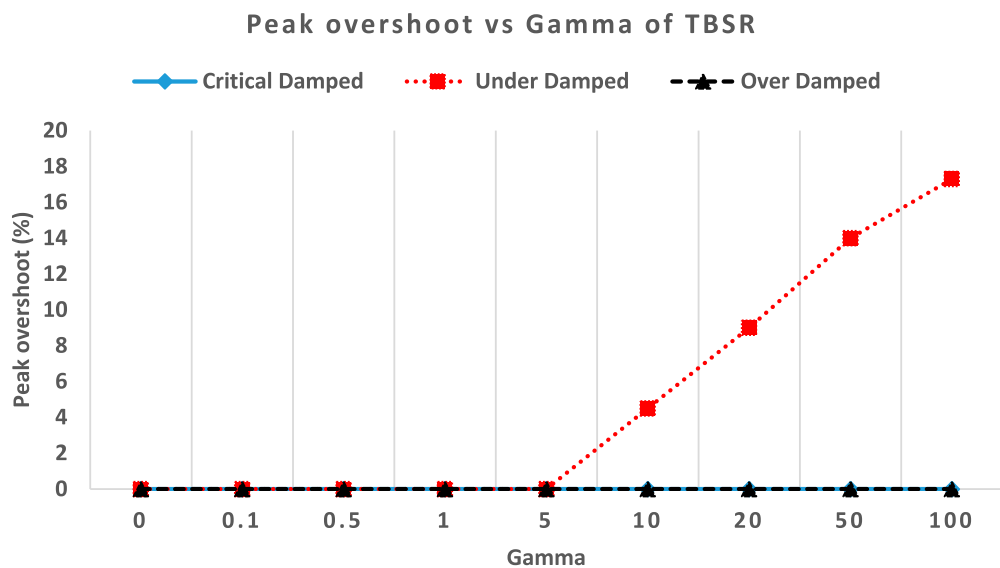


Figure 26. Comparison of MRAC TBSR for different values of gamma with peak overshoot.

7. Comparison of controller performance for different values of adaption gain gamma

Adaption gain gamma is the key parameter which governs the performance of the plant. All the three plants TBSC, TBSR, and TBSC + TBSR, are simulated with three different reference models, and in each case, t_r , t_s , and m_p values are measured. Each performance specification is plotted with varying gamma in the range of 0 to 100 for different MRAC models as critically, under, and overdamped conditions. The variations in these parameters are shown in Figures 19–27.

While Figures 19–21 show the rise time performance parameter plot of TBSC, TBSR, and TBSC + TBSR plant for different adaption gain gamma with different reference models, such as critically, under, and overdamped. It is observed that rise time for critical, under, and overdamped reference models are somewhat the same, and as gamma increases and rise time goes down.

The settling time performance parameter of TBSC, TBSR, and TBSC + TBSR plant is plotted in

Figures 22–24 for different adaption gain gamma with different reference models, such as critically, under, and overdamped.

The peak overshoot performance parameter of TBSC, TBSR, and TBSC + TBSR plant is plotted in Figures 25–27 for different adaption gain gamma with different reference models, such as critically, under, and overdamped.

8. Testing of systems adaptations for square wave pulses

The main aim of using model reference adaptive controller is that plant response should follow the reference model. By observing Tables 12–14, the reference model that gives the best performance is critically damped. To check this, a train of square wave pulses is applied. This has an ON period of 25 s and an OFF period of 25 s. For this square wave pulse, the adaptation of TBSC, TBSR, and TBSC + TBSR has been tested, and performance plots are given as below:

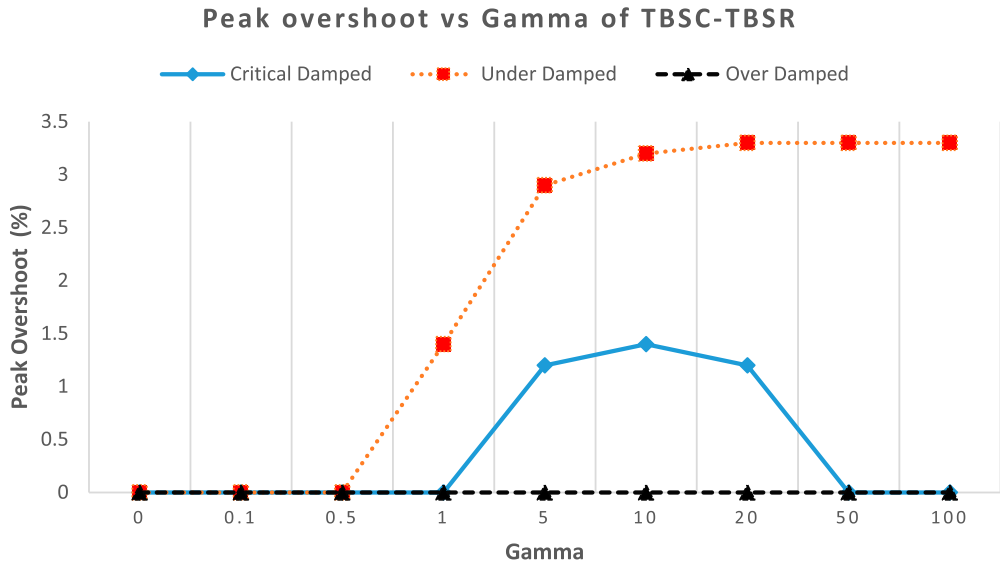


Figure 27. Comparison of MRAC TBSC-TBSR for different values of gamma with peak overshoot.

8.1. Adaptive performance of VAR generator (TBSC) for square wave input with critically damped

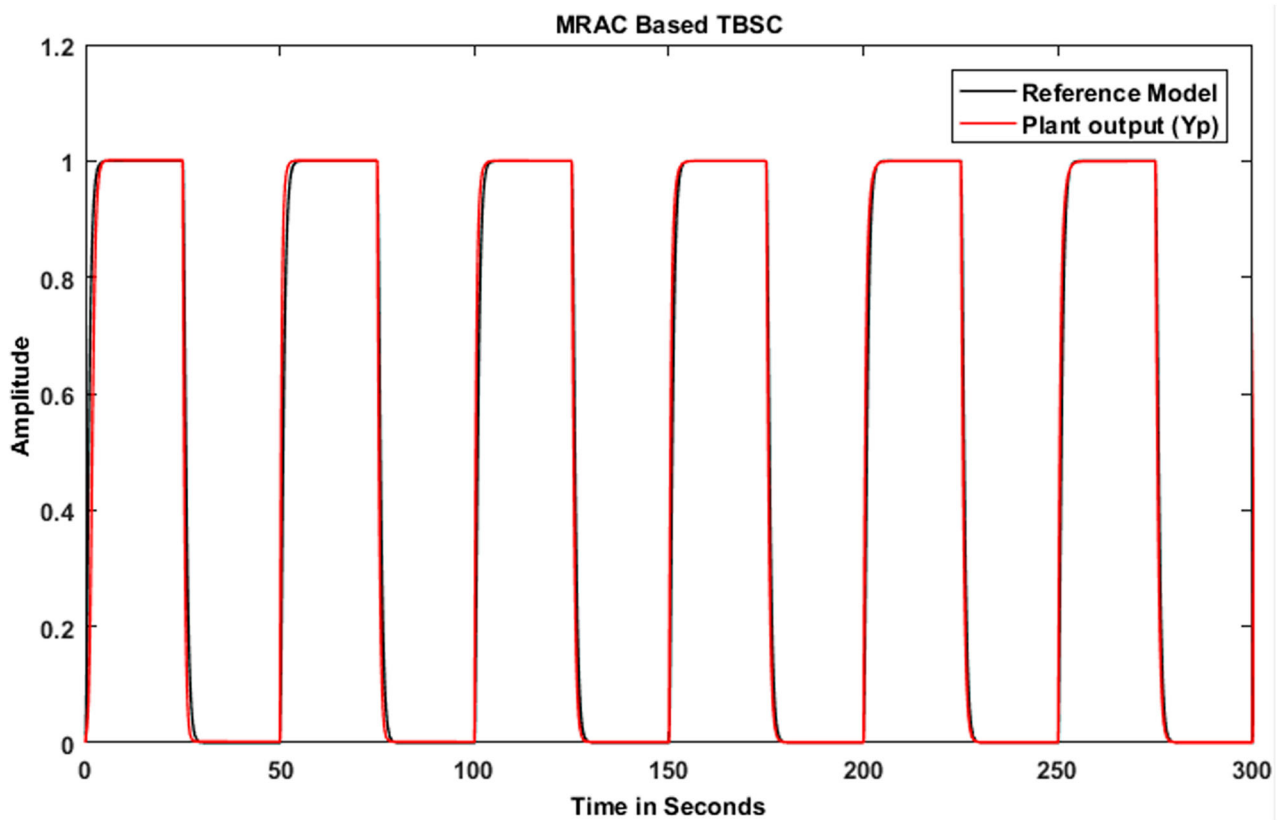


Figure 28. Adaptive performance of VAR generator (TBSC) for square wave input with critically damped.

8.2. Adaptive performance of VAR absorber (TBSR) for square wave input with critically damped

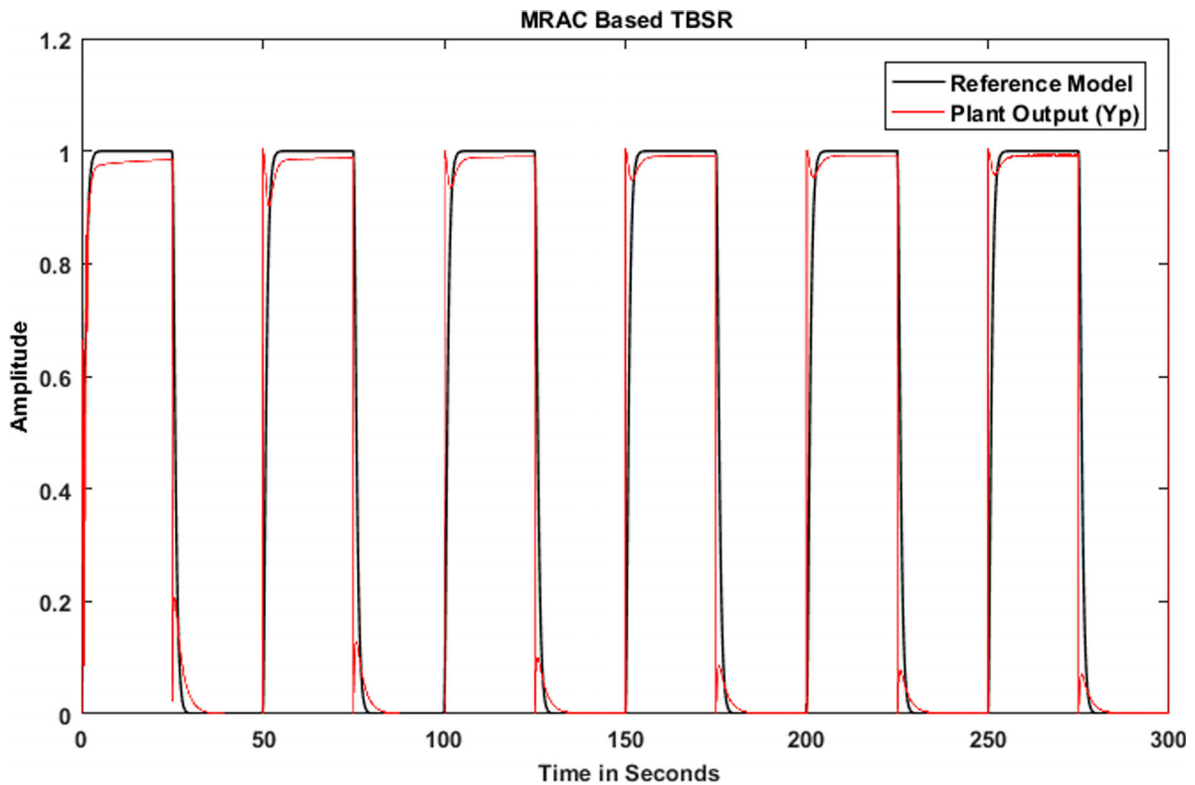


Figure 29. Adaptive performance of VAR absorber (TBSR) for square wave input with critically damped.

8.3. Adaptive performance of VAR generator and absorber (TBSC + TBSR) for square wave input with critically damped

By observing the Figures 28–30 and Tables 15–17, it is noted that as time progresses the performance parameter such as t_r , t_s and m_p improves considerably, means the system is adapting towards the reference model.

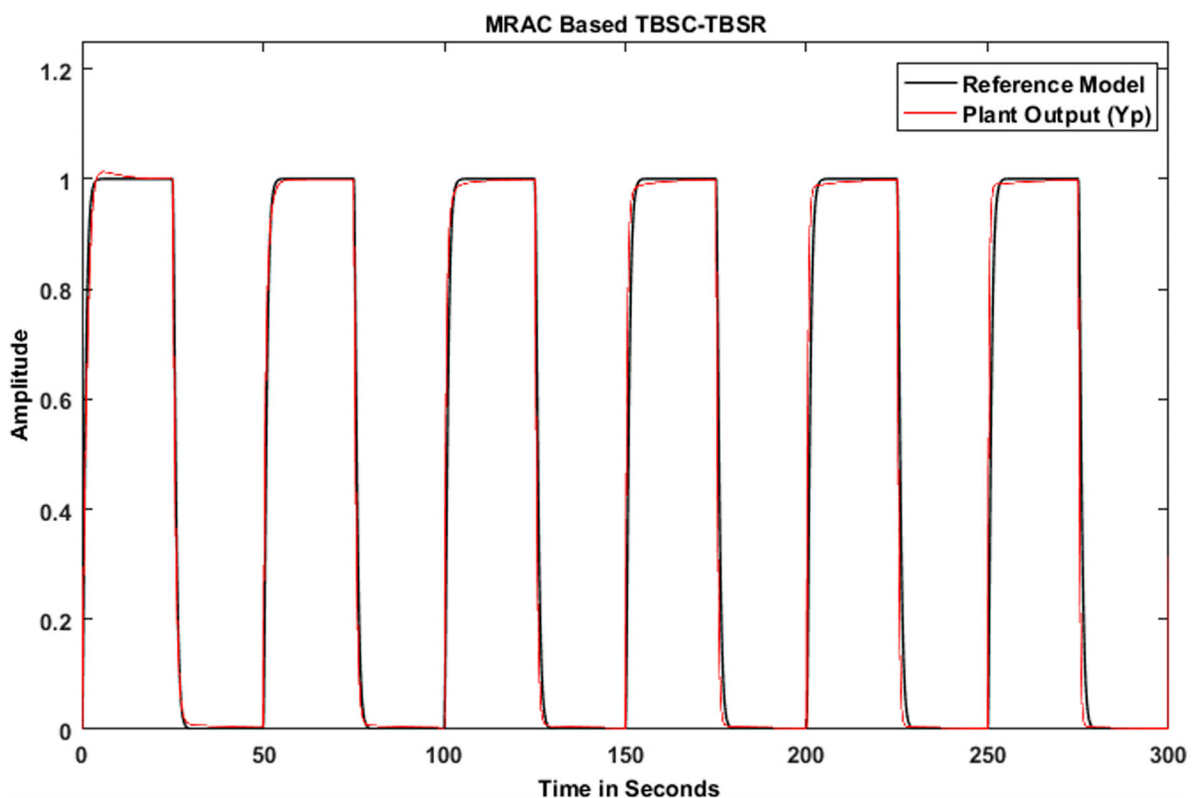


Figure 30. Adaptive performance of VAR generator and absorber (TBSC + TBSR) for square wave input with critically damped.

Table 15. The adaption performance Parameter of VAR generator (TBSC) for critically damped reference model with square wave input.

Instant	t_r in sec	t_s in sec	m_p in %
Critical damped			
At (0.0 sec.)	02.80	04.80	Nil
At (50.0 sec)	01.37	04.50	Nil
At (200.0 sec)	00.93	03.39	Nil

9. Significance improvement and comparison of the performance parameters

The performance of a static var compensator system mainly depends upon the control action taken by the controller. The parameter considered in this regard is t_r , t_s , and m_p . In the rapid expansion of power systems, a load is becoming nonlinear in nature day by day. Also, because of large variations in the environmental condition such as temperature, humidity, and aging, the inductance and capacitance of the plant goes on degrading their rated values which leads to the development of adaptive controllers. These adaptive controllers are most suitable in case of change in loads, inertia, and drastic change in system parameters, unpredictable loads, faults, and disturbance. Several papers are reported regarding the MRAC with auto-tuning of PID controllers and fuzzy-neural –PID. To enhance the performance of SVC by the model reference adaptive controller based self-tuning adaptive neural controller was discussed in [40]. A comparative review of an adaptive control scheme for improving the system dynamics was considered in [41].

In [40], the performance enhancement parameters such as t_r , t_s , and m_p of compensating variables are evaluated by considering a stepped load concept. The controller used as a model reference adaptive controller based on self-tuning PID. In this paper, voltage responses for different stepped loading conditions are plotted. Two adaptive controllers used for comparison are ANN and ANN-PID. The rise time increases from 0.487 sec to 0.863 sec. While settling time varies between 1.0848 sec to 3.684 sec, and peak overshoot varies from 5.11–18.82%. Comparing these results with the method proposed in this paper is much better. Also, in [42,43], the effect of adaptation gain on the second-order system was considered. By observing the time response plots for output shows a considerably larger time duration is taken for performance specification. Also, it is observed that the overshoot results in oscillation due to these system voltage oscillations, which may lead to a dangerous situation. By choosing the proper reference model, these oscillations are suppressed in this paper.

In this paper, the value of peak overshoot is zero, which indicates no oscillations. A typical case of square input after 50 sec shows the rise time as 0.014, and after

Table 16. Adaptive performance of VAR absorber (TBSR) for critically damped reference model with square wave input.

Instant	t_r in sec	t_s in sec	m_p in %
Critical damped			
At (0.0 sec.)	01.860	> 25.00	Nil
At (50.0 sec)	00.014	> 25.00	Nil
At (200.0 sec)	00.006	> 25.00	Nil

Table 17. Adaptive performance of VAR generator and absorber (TBSC + TBSR) for critically damped reference model with square wave input

Instant	t_r in sec	t_s in sec	m_p in %
Critical damped			
At (0.0 sec.)	02.55	21.00	00.01
At (50.0 sec)	01.87	20.50	Nil
At (200.0 sec)	00.91	15.70	Nil

200 sec, it gives 0.006 sec. A complete analysis of performance specifications is given based on adaptation gain (γ) variation between 0-100. The MRAC scheme is most suitable in the case of varying the plant parameters and nonlinear types of loads. The performance of the system mainly depends on the adaptation gain γ . The value of the adaptation gain to be chosen carefully to obtain the best performance.

10. Conclusion

A reactive power compensator as SVC having four switched capacitor banks (TBSC) in binary weightage is designed. The mechanism of the closed-loop control is achieved. The TBSC compensator is acting as a coarse controller. There will be an error of lowest step value of TBSC bank takes place. The error in compensation is $\frac{1}{24} * 100 = 6.25\%$, or conversely, the net compensation has done due to coarse control action is 93.75%. This leading reactive power error is once again compensated by lagging reactive power absorbed by a binary-weighted reactor bank divided into four steps (TBSR). This part of the system is acting as a fine control. So, in all, the number of a switched steps becomes eight, and error in compensation becomes $\frac{1}{28} = 0.39\%$ or net compensation takes place as 99.61%. Both these compensators are connected in cascade form, and simulation results are presented.

A feedforward MRAC is used to improve the system performance, and performance specifications are evaluated for different reference models such as critical, over, and underdamped conditions. The performance specifications, such as t_r , t_s , and m_p , are tabulated by using MRAC with varying adaptation gain. Performance parameters for all the three systems with the mathematical model identified are analyzed and listed. These performance parameters are obtained for different reference models as well as for different adaptation gain γ . The combined TBSC + TBSR with MRAC works well and adapts, giving the improved

performance in time response specifications as time progresses. This has also been shown by using a square wave train of pulses as input and improved rise time and settling time parameters tabulated. This system shows a considerable improvement in the response time, which ultimately, fast compensation of reactive power takes place.

Disclosure statement

No potential conflict of interest was reported by the author(s).

Funding

Shivaji University, Kolhapur, funds this project under Research Initiation Scheme, Maharashtra, INDIA. Sanction letter reference no.: [SU/C&U.D.Section/50/397], dated 21st July 2018.

ORCID

Swapnil D. Patil  <http://orcid.org/0000-0003-4466-7256>
 Renuka A. Kachare  <http://orcid.org/0000-0002-3656-070X>
 Anwar M. Mulla  <http://orcid.org/0000-0003-1025-8892>
 Dadgonda R. Patil  <http://orcid.org/0000-0003-2884-4160>

References

- [1] Gandoman FH, Ahmadi A, Sharaf AM, et al. Review of FACTS technologies and applications for power quality in smart grids with renewable energy systems. *Renew Sustainable Energy Rev*, Elsevier. 2018;82: 502–514. doi:10.1016/j.rser.2017.09.062.
- [2] Gayatri MTL, Parimi AM, Pavan Kumar AV. A review of reactive power compensation techniques in micro-grids. *Renew Sustainable Energy Rev*, Elsevier. 2018: 1030–1036. doi:10.1016/j.rser.2017.08.006.
- [3] Badal FR, Das P, Sarker SK, et al. A survey on control issues in renewable energy integration and microgrid. *Prot Control Mod Power Syst*, Springer. 2019: 1–27. doi:10.1186/s41601-019-0122-8.
- [4] Hemeida MG, Rezk H, Hamada MM. A comprehensive comparison of STATCOM versus SVC-based fuzzy controller for stability improvement of wind farm connected to multi-machine power system. *Electr Eng*, Springer. 2017: 1–7. doi:10.1007/s00202-017-0559-6.
- [5] Khaledian A, Aliakbar Golkar M. A new power sharing control method for an autonomous microgrid with regard to the system stability. *Automatika*, Taylor and Francis. 2018;59(1):87–93. doi:10.1080/00051144.2018.1501462.
- [6] Wang D, Glavic M, Wehenkel L. A new MPC scheme for damping wide-area electromechanical oscillations in power systems. 2011 IEEE Trondheim PowerTech. *June 2011*:1–7, 19–23.
- [7] Wang L, Cheung H, Hamlyn A, et al. Model prediction adaptive control of inter-area oscillations in multi-generators power systems. *Power Energy Soc Gen Meeting, 2009. PES '09. IEEE*. 26–30 July 2009;1:1–7.
- [8] Bo G, Hiskens IA. Two-stage model predictive control for voltage collapse prevention. 40th North American Power Symposium, 2008, 28–30 Sept. 2008.
- [9] Lin J, Kumar R, Elia N. Model predictive control-based real-time power system Protection schemes. *IEEE Trans Power Syst*. *May 2010*;25(2):988–998.
- [10] Maki O, Turunen J, Seppänen J, et al. Robustness and performance of a multi-objective model predictive static var compensator controller. *Power Systems Computation Conference (PSCC)*, IEEE, 2016. doi:10.1109/PSCC.2016.7540978
- [11] Mi Y, Ma C, Fu Y, et al. The SVC additional adaptive voltage controller of Isolated Wind-Diesel power system based on double sliding mode optimal strategy. *IEEE Trans Sustain Energy*. doi:10.1109/TSSTE.2017.2713700
- [12] Kassem M, Abdelaziz AY. Reactive power control for voltage stability of standalone hybrid wind-diesel power system based on functional model predictive control. *IET Renew Power Gener*. *Nov. 2014*;8(8): 887–899.
- [13] Bai J, Erlich I. A multi-objective predictive controller for power oscillation damping and voltage control in power system. *ScienceDirect, IFAC Papers Online*. 2018;51–28:398–403. Elsevier, 398–403. doi:10.1016/j.ifacol.2018.11.735
- [14] Gong B, Hiskens IA. Two-Stage model predictive control for voltage collapse prevention. *IEEE Xplore*. doi:10.1109/NAPS.2008.5307302
- [15] Bansal RC. Automatic reactive-power control of Isolated Wind-Diesel hybrid power systems. *IEEE Trans Ind Electron*. *Jun. 2006*;53(4):1116–1126.
- [16] Bansal RC, Bhatti TS, Kothari DP. A novel mathematical modeling of induction generator for reactive power control of isolated hybrid power systems. *Int J Model Simul*. *May 2004*;24(1):1–7.
- [17] Banerjee A, Mukherjee V, Ghoshal SP. Intelligent fuzzy-based reactive power compensation of an isolated hybrid power system. *Int J Elec Power*. *May. 2014*;57:164–177.
- [18] Banerjee A, Mukherjee V, Ghoshal SP. Modeling and seeker optimization-based simulation for intelligent reactive power control of an isolated hybrid power system. *Swarm Evol Comput*. *Dec. 2013*;13:85–100.
- [19] Salam F, Mosaad MI. 'A comparison between MPC and optimal PID controllers: case studies.' *IET Conf., Michael Faraday IET Int. Summit: MFIIS-2015, Kolkata, India, 2015*, pp. 59–65.
- [20] Patil SD, Mulla AM, Gudaru U, et al. "An Innovative Transient Free TBSC Compensator with Closed Loop Control for Fast Varying Dynamic Load," *Proceedings of WCECS 2014, Vol I 23-25 October 2014, San Francisco, USA*.
- [21] Patil S, Pawar S, Mulla A, et al. FC-TBSR compensator for reactive power compensation and voltage swell mitigation. In: *Favorskaya M, Mekhilef S, Pandey R, Singh N, editors. Innovations in Electrical and Electronic engineering. lecture notes in Electrical Engineering*, vol 661. Singapore: Springer; 2021. doi:10.1007/978-981-15-4692-1_2
- [22] Patil S, Shende K, Patil D, et al. TBSC compensator. In: *Ao SI, Kim H, Amouzegar M, editors. Transactions on engineering technologies. WCECS 2015*. Singapore: Springer; 2017, Print ISBN 978-981-10-2716-1, Online ISBN 978-981-10-2717-8. p. 305–318. doi:10.1007/978-981-10-2717-8_22
- [23] Patil SD, Kachare RA, Mulla AM, et al. Performance enhancement of modified SVC as a Thyristor binary switched capacitor and reactor banks by using different adaptive controllers. *J King Saud Univ - Eng Sci*, Elsevier. 2021. ISSN 1018-3639. doi:10.1016/j.jksues.2021.06.006.
- [24] Brekken TKA, Yokochi A, Von Jouanne A, et al. Optimal energy storage sizing and control for wind

- power applications. *IEEE Trans Sustain Energy*. Jan. 2011;2(1):69–77.
- [25] Hamidi V, Li F, Yao L. Value of wind power at different locations in the grid. *IEEE Trans Power Del*. Apr. 2011;26(2):526–537.
- [26] Mosaad MI. Model reference adaptive control of STATCOM for grid integration of wind energy systems. *IET Electr Power Appl* 2018;12(5):605–613. doi:10.1049/iet-epa.2017.0662.
- [27] Saxena NK. Voltage control by optimized participation of reactive power compensation using fixed capacitor and STATCOM. Springer Nat Switzerland AG. 2020. doi:10.1007/978-3-030-34050-6_13.
- [28] Djagarov NF, Grozdev ZG, Bonev MB, et al. An adaptive control of static var compensator on power systems. *IASME/WSEAS International Conference on Energy & Environmental Systems, Chalkida, Greece, May 8-10, 2006* pp151–157.
- [29] Naderipur A, Abdul-Malek Z, Gandoman FH, et al. Optimal designing of static var compensator to improve the voltage profile of power system using fuzzy logic control. *Energy*, Published by Elsevier 2019, Science Direct. doi:10.1016/j.energy.2019.116665.
- [30] Wei F, Tianqi L, Xingyuan L, et al. Summary of analysis and control methods of static var compensator's operating characteristics. *Power Syst Prot Control*, Nov. 16, 2014. 2018;42(22). doi:1674-3415(2014)22-0147-08.
- [31] Finotti C, Gaio E, Song I, et al. Improvement of the dynamic response of the ITER reactive power compensation system. *Fusion Eng Design*, Elsevier. 2018. doi:10.1016/j.fusengdes.2015.05.044.
- [32] Asban MR, Aghaei J, Niknam T, et al. Designing static VAR compensator capacity to enhance power quality in electric arc furnaces. *Simulation*. 2017;93(6):515–525.
- [33] Maiti D, Mukhopadhyay S, Biswas SK. Three phase thyristor controlled reactor using two sets of delta connected switches with low current harmonics. *IET Power Electron*. 2019;12:4016–4022. doi:10.1049/iet.pel.2018.5020.
- [34] Das S, Chatterjee D, Goswami SK. A reactive power compensation scheme for unbalanced four wire system using virtual Y-TCR model. *IEEE Trans Ind Electron*. April 2018;65(4):3210–3219. doi:10.1109/TIE.2017.2758720.
- [35] Gelen A, Yalcinoz T. Analysis of TSR-based SVC for a three-phase system with static and dynamic loads. *Turk J Elec Eng & Comp Sci*. 2010;18(2). doi:10.3906/elk-0907-138.
- [36] Gelen A, Yalcinoz T. Experimental studies of a scaled-down TSR-based SVC and TCR-based SVC prototype for voltage regulation and compensation. *Turk J Elec Eng Comp Sci*. 2010;18(2). doi:10.3906/elk-0907-138.
- [37] Wang L, Lam CS, Wong MC. An unbalanced control strategy for a thyristor controlled LC-coupling hybrid active power filter (SVC–HAPF) in three-phase three-wire systems. *IEEE Trans Power Electron*. Feb. 2017;32(2):1056–1069.
- [38] Dixon J, del Valle Y, Orchard M, et al. A full compensating system for general loads, based on a combination of thyristor binary compensator, and a PWM-IGBT active power filter. *IEEE Trans Ind Electron*. Oct. 2003;50(5):982–989.
- [39] Astrom KJ, Wittenmark B. *Adaptive controllers*. Singapore: Pearson Education Asia; 2001.
- [40] Abood AA, Tuaimah FM, Maktoof AH. Modeling of SVC controller based on adaptive PID controller using neural networks. *Int J Comput Appl (0975–8887)*. 2018;59(6):9–16.
- [41] Swarnkar P, Jain SK, Nema RK. Adaptive control Schemes for improving the control system dynamics: A review. *IETE Tech Rev*. 2014;31(1):17–33.
- [42] Swarnkar P, Jain S, Nema RK. Effect of adaptation gain in model reference adaptive controlled second order system. *Int J ETASR*. 2013;1(3):705.
- [43] Swarnkar P, Jain S, Nema RK. Comparative analysis of MIT rule and Lyapunov rule in model reference adaptive control scheme. *Int J Innov Syst Des Eng*. 2012;2(4):15462.